J. Fluid Mech. (1997), *vol.* 353, *pp.* 83–114. Printed in the United Kingdom

© 1997 Cambridge University Press

Effects of pressure gradients on turbulent premixed flames

By DENIS VEYNANTE† AND THIERRY POINSOT‡

Center for Turbulent Research, Stanford University and NASA Ames Research Center, Stanford, CA 94035, USA

(Received 29 July 1996 and in revised form 7 July 1997)

In most practical situations, turbulent premixed flames are ducted and, accordingly, subjected to externally imposed pressure gradients. These pressure gradients may induce strong modifications of the turbulent flame structure because of buoyancy effects between heavy cold fresh and light hot burnt gases. In the present work, the influence of a constant acceleration, inducing large pressure gradients, on a premixed turbulent flame is studied using direct numerical simulations.

A favourable pressure gradient, i.e. a pressure decrease from unburnt to burnt gases, is found to decrease the flame wrinkling, the flame brush thickness, and the turbulent flame speed. It also promotes counter-gradient turbulent transport. On the other hand, adverse pressure gradients tend to increase the flame brush thickness and turbulent flame speed, and promote classical gradient turbulent transport. As proposed by Libby (1989), the turbulent flame speed is modified by a buoyancy term linearly dependent on both the imposed pressure gradient and the integral length scale l_t.

A simple model for the turbulent flux $\widetilde{u''c''}$ is also proposed, validated from simulation data and compared to existing models. It is shown that turbulent premixed flames can exhibit both gradient and counter-gradient transport and a criterion integrating the effects of pressure gradients is derived to differentiate between these regimes. In fact, counter-gradient diffusion may occur in most practical ducted flames.

1. Introduction

Most ducted turbulent flames are subjected to external pressure gradients. Compared to 'free' flames, i.e. turbulent flames without externally imposed pressure gradients, the combination of the external pressure gradients with the large density changes found in premixed flames may lead to strong modifications of the flame structure. These modifications are mainly due to the differential buoyancy effects between cold heavy reactants and hot light products. They affect turbulent transport along with many characteristics of the flame itself, such as flame speed, thickness, wrinkling, and local structure. Pressure gradients are also a key mechanism for the counter-gradient turbulent transport described below. Accordingly, studying the effects of pressure gradients on premixed turbulent flames is an important issue both for fundamental understanding of turbulent combustion and for modelling.

Using the assumption of single-step chemistry, the mass fractions of the reactive

† Permanent address: Laboratoire E.M2.C., CNRS - Ecole Centrale Paris, France.
‡ Permanent address: Institut de Mécanique des Fluides de Toulouse and CERFACS, France.

species are all linearly related (Williams 1985) and may be expressed in terms of a single reduced mass fraction: the reaction progress variable c. The progress variable ranges from zero to unity in the fresh and fully burnt gases, respectively. Using the classical Favre decomposition, a quantity q can be split into a mass-weighted mean, $\widetilde{q} \equiv \overline{\rho q}/\overline{\rho}$, and a turbulent fluctuation, q''. The transport equation for the mean reaction progress variable $\widetilde{c}$ may be written as

$$\frac{\partial \overline{\rho}\widetilde{c}}{\partial t} + \frac{\partial \overline{\rho}\widetilde{u}_i\widetilde{c}}{\partial x_i} + \frac{\partial \overline{\rho u_i'' c''}}{\partial x_i} = -\overline{\frac{\partial \mathscr{J}_k}{\partial x_k}} + \overline{\dot{\omega}}_c \tag{1.1}$$

where ρ is the mass density, u_i is the flow velocity, $\mathscr{J}_k$ is the molecular diffusion flux, $\dot{\omega}_c$ is the volumetric production rate of the chemical reaction, and the overbar denotes conventional Reynolds ensemble-averaging. Equation (1.1) has the form of a standard turbulent transport equation where the rate of change of $\widetilde{c}$ results from a balance between convection by the mean flow, convection by the turbulent flow, molecular diffusion, and chemical reaction. The contribution of molecular diffusion is usually neglected for high-Reynolds-number flows. In (1.1), two terms need to be modelled: the mean reaction rate $\overline{\dot{\omega}_c}$ and the turbulent transport $\overline{\rho u_i'' c''}$ terms. The first term has received considerable attention in recent years and various models have been derived and incorporated into practical codes for turbulent combustion. The second term, however, has received considerably less attention and is generally described with a simple classical gradient eddy-viscosity model:

$$\overline{\rho u_i'' c''} = \overline{\rho}\widetilde{u_i'' c''} = -\frac{\mu_t}{\sigma_c}\frac{\partial \widetilde{c}}{\partial x_i} \tag{1.2}$$

where μ_t denotes the turbulent dynamic viscosity and σ_c a turbulent Schmidt number.

Both theoretical and experimental research (Bray *et al.* 1981; Bray, Moss & Libby 1982; Shepherd, Moss & Bray 1982) have found evidence of counter-gradient transport in some turbulent flames: in these flames the turbulent flux $\overline{\rho u_i'' c''}$ and the $\widetilde{c}$ gradient $\partial\widetilde{c}/\partial x_i$ have the same sign in opposition with the prediction of (1.2). This is generally due to the differential effect of pressure gradients on cold reactants and hot products. Recent studies based on direct numerical simulations of turbulent premixed flames without externally imposed pressure gradients (Trouvé *et al.* 1994; Rutland & Cant 1994) have confirmed that counter-gradient diffusion was found in simulations, but that classical gradient diffusion was also possible. A criterion indicating the presence of gradient or counter-gradient diffusion in atmospheric flames has been derived by Veynante *et al.* (1997). This criterion leads to a reduced number called N_B:

$$N_B = \frac{\tau}{2\alpha(u'/s_l^0)} \tag{1.3}$$

where s_l^0 is the laminar flame speed, u' is the RMS turbulent velocity, τ is the heat release factor defined as $\tau = T_b/T_u - 1$, with T being the temperature and indices u and b referring to the fresh and burnt gases, respectively. The term α is an efficiency function of order unity, introduced by Veynante *et al.* (1997) to take into account the reduced ability of small turbulent vortices to affect the flame front. This function is plotted on figure 1. For low values of N_B, typically $N_B \leqslant 1$ (flames in relatively large turbulence intensity), gradient diffusion is obtained. For large values of N_B counter-gradient diffusion occurs. In fact, counter-gradient turbulent diffusion is promoted by heat release and thermal expansion (increasing values of τ) whereas increased turbulence intensity tends to induce gradient transport.

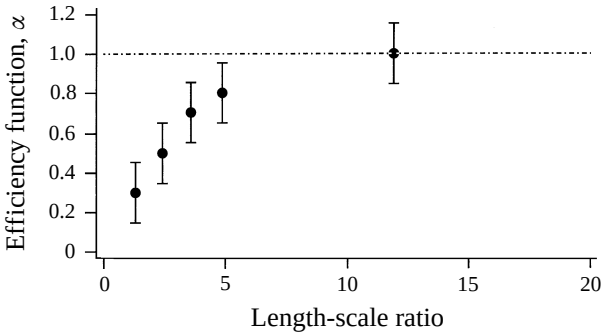

FIGURE 1. A DNS-based estimate of the efficiency function α, introduced by Veynante *et al.* (1997) to take into account the reduced ability of small turbulent vortices to affect the flame front. The function α is plotted as a function of the length-scale ratio l_t/δ_l^0 where l_t is the turbulence integral length scale and δ_l^0 the thermal thickness of the laminar flame.

The work of Veynante *et al.* (1997) was performed for free flames without externally imposed pressure gradients or volume forces, such as gravity. Since turbulent transport in flames appears to be controlled by a dynamic balance between fresh and burnt gases, confined flames subjected to strong pressure gradients should exhibit a large sensitivity to these gradients. For example, we expect that imposing a pressure gradient on a turbulent flame exhibiting counter-gradient diffusion may lead to a gradient-diffusion situation. This change may affect the flame brush thickness, the turbulent flame speed and finally the complete structure of the turbulent flame brush, as described in a number of papers such as Masuya & Libby (1981); Bray *et al.* (1982).

Our objective in this study is to explore the effects of pressure gradients on premixed turbulent flames using direct numerical simulations. We will first recall the physics of this phenomenon and how pressure gradients may be included in a simulation for reacting flows in §2. We will also describe the most general theory to treat the problem, i.e. the Bray–Moss–Libby formulation. The simulation used for this work will be described in §3. Section 4 will present the structure of laminar flames submitted to pressure gradients. Section 5 will present results for turbulent flames. Finally, §6 will describe a model for the turbulent flux incorporating the effects of pressure gradients and a comparison with experimental results by Shepherd *et al.* (1982).

2. Pressure gradients in premixed flames

2.1. *The Bray–Moss–Libby approach for turbulent transport*

Bray, Champion & Libby (1989) have proposed a simple algebraic closure for the reaction term $\overline{\dot{\omega}}_c$ in (1.1), but focus their attention on the turbulent transport term $\overline{\rho u_i'' c''}$. In the Bray-Moss-Libby (BML) approach, the flame is analysed as a thin flame sheet, or 'flamelet', separating fresh reactants ($c = 0$) and fully burnt products ($c = 1$). This assumption leads to a bimodal probability density for the progress variable c and the turbulent flux is then expressed, according to Bray (1980), as:

$$\overline{\rho u_i'' c''} = \overline{\rho} \widetilde{c}(1 - \widetilde{c})(\overline{u}_{ib} - \overline{u}_{iu}) \tag{2.1}$$

where $\overline{u}_{iu}$ and $\overline{u}_{ib}$ are the conditional mean velocities within the unburnt and burnt gases, respectively. The occurrence of counter-gradient transport may be easily ex-

plained from this expression. Let us consider a left-travelling flame in the x_i-direction ($\partial\widetilde{c}/\partial x_i > 0$). Thermal expansion and the associated flow acceleration through the flame, along with favourable buoyancy and/or pressure gradients, will tend to make $\overline{u}_{ib}$ larger than $\overline{u}_{iu}$, thereby promoting counter-gradient turbulent diffusion of $\widetilde{c}$, resulting in $\overline{\rho}\widetilde{u_i''c''} > 0$. Under the BML approach, the second and third turbulent moments such as $\overline{\rho}\widetilde{u_i''u_j''}$, $\overline{\rho}\widetilde{u_i''u_j''}c''$, and $\overline{\rho}u_i''\widetilde{u_j''u_k''}$ may be directly expressed as functions of conditioned quantities in fresh and in burnt gases. Nevertheless, conditional quantities such as $(\overline{u}_{ib} - \overline{u}_{iu})$ are difficult to close and an alternative approach must be pursued for estimating the turbulent transport $\overline{\rho}\widetilde{u_i''c''}$. A simple algebraic closure based on the eddy-viscosity concept cannot be used here. In the BML model, closure is achieved by a transport equation for $\overline{\rho u_i''c''}$ (Bray 1980, 1990; Bray *et al.* 1989). A brief derivation of this equation is provided here, including a constant volume force F_i^v and a constant acceleration Γ_i. These terms will both induce a mean pressure gradient in the flow as shown below. Start from the momentum equation

$$\frac{\partial \rho u_i}{\partial t} + \frac{\partial \rho u_i u_j}{\partial x_j} = -\frac{\partial P}{\partial x_i} + F_i^v + \rho\Gamma_i + \frac{\partial \tau_{ik}}{\partial x_k} \tag{2.2}$$

and the equation for the progress variable c

$$\frac{\partial \rho c}{\partial t} + \frac{\partial \rho u_i c}{\partial x_j} = -\frac{\partial \mathscr{J}_k}{\partial x_k} + \dot{\omega}_c \tag{2.3}$$

where P, τ_{ij} and $\mathscr{J}_k$ are respectively the pressure, the viscous stress tensor and the molecular diffusive flux of c. Multiplying (2.2) by c and (2.3) by u_i, then adding and averaging the two resulting equations leads to a transport equation for $\overline{\rho}\widetilde{u_i c}$. In a similar way, adding the averaged version of (2.2) multiplied by $\widetilde{c}$ and the averaged form of (2.3) multiplied by $\widetilde{u}_i$ leads to a transport equation for $\overline{\rho}\widetilde{u}_i\widetilde{c}$. Subtracting the two resulting equations provides a transport equation for the turbulent flux $\overline{\rho}\widetilde{u_i''c''}$:

$$\begin{aligned}\underbrace{\frac{\partial \overline{\rho}\widetilde{u_i''c''}}{\partial t}}_{\text{(I)}} + \underbrace{\frac{\partial \overline{\rho}\widetilde{u}_j\widetilde{u_i''c''}}{\partial x_j}}_{\text{(II)}} = &- \underbrace{\frac{\partial \overline{\rho}\widetilde{u_j''u_i''c''}}{\partial x_j}}_{\text{(III)}} - \underbrace{\overline{\rho}\widetilde{u_i''u_j''}\frac{\partial \widetilde{c}}{\partial x_j}}_{\text{(IV)}} - \underbrace{\overline{\rho}\widetilde{u_j''c''}\frac{\partial \widetilde{u}_i}{\partial x_j}}_{\text{(V)}} - \underbrace{\overline{c''}\frac{\partial \overline{p}}{\partial x_i}}_{\text{(VI)}} \\ &- \underbrace{\overline{c''\frac{\partial p'}{\partial x_i}}}_{\text{(VII)}} - \underbrace{\overline{u_i''\frac{\partial \mathscr{J}_k}{\partial x_k}}}_{\text{(VIII)}} - \underbrace{\overline{c''\frac{\partial \tau_{ik}}{\partial x_k}}}_{\text{(IX)}} + \underbrace{\overline{\rho}\widetilde{u_i''\dot{\omega}_c}}_{\text{(X)}} + \underbrace{\overline{c''}F_i^v}_{\text{(XI)}}.\end{aligned} \tag{2.4}$$

Bray *et al.* (1981) studied each term in (2.4) and proposed some approximations. For example, they explored the role of the mean pressure gradient term (VI) assuming that this term is so large that only cross-dissipation terms (VIII and IX) can provide a balance, leading to a turbulent flux directly proportional to the pressure gradient. All terms in (2.4) may be extracted from direct numerical simulations (Trouvé *et al.* 1994; Veynante *et al.* 1997) to validate these analysis.

Two main comments arise concerning (2.4). First, the mean pressure gradient appears explicitly in the source term (VI) ($\overline{c''}\partial\overline{p}/\partial x_i$). Under the BML analysis, $\overline{c''}$ may be easily closed (Masuya & Libby 1981):

$$\overline{c''} = \overline{c} - \widetilde{c} = \tau\frac{\widetilde{c}(1-\widetilde{c})}{1+\tau\widetilde{c}} \tag{2.5}$$

which is exact for an infinitely thin flame front. This quantity is always positive so that $\partial\overline{P}/\partial x_i$ controls the sign of (VI): a pressure decrease from fresh to burnt gases

tends to promote counter-gradient diffusion (or positive values of the turbulent flux $\overline{\rho}\widetilde{u_i''c}$).

Another important feature deals with volume and buoyancy forces. A constant volume force F_i^v leads to a source term in (2.4), with a similar form for the pressure gradient term, whereas a constant acceleration force Γ_i does not. However, the introduction of F_i^v or Γ_i also has a direct influence on the mean pressure gradient $\partial\overline{P}/\partial x$ (term VI) and terms (VI) and (XI) should be grouped together to describe the effect of F_i^v or Γ_i. We start from the averaged momentum transport equation:

$$\frac{\partial\overline{\rho}\widetilde{u_i}}{\partial t}+\frac{\partial\overline{\rho}\widetilde{u_i}\widetilde{u_j}}{\partial x_j}+\frac{\partial\overline{\rho}\widetilde{u_i''u_j''}}{\partial x_j}=-\frac{\partial\overline{P}}{\partial x_i}+F_i^v+\overline{\rho}\Gamma_i+\frac{\partial\overline{\tau}_{ik}}{\partial x_k}. \tag{2.6}$$

For sufficiently large volume and/or buoyancy forces, the leading-order terms in (2.6) are these forces and the mean pressure gradient so that the hydrostatic approximation provides a good estimate of the pressure gradient:

$$\frac{\partial\overline{P}}{\partial x_i}=F_i^v+\overline{\rho}\Gamma_i. \tag{2.7}$$

Therefore, to first order, term (VI + XI) becomes

$$-\overline{c''}\left(\frac{\partial\overline{P}}{\partial x_i}-F_i^v\right).=-\overline{c''}\overline{\rho}\Gamma_i. \tag{2.8}$$

Both F_i^v and Γ_i induce a mean pressure gradient in the flow field (see (2.2)). However, only Γ_i will directly affect the balance of $\overline{\rho}\widetilde{u_i''c''}$ (2.4) because, contrary to a constant acceleration, a constant volume force does not introduce buoyancy phenomena. Accordingly, our study of the influence of the mean pressure gradient on turbulent transport will be conducted using a constant acceleration Γ_i.

2.2. *Physical and numerical issues related to pressure gradients in flames*

Theoretical models indicate that both normal and tangential pressure gradients influence turbulent flames. Masuya & Libby (1981) have studied confined oblique flames and have shown that, for a given pressure gradient, turbulent transport in normal and transverse directions are correlated. As a first step, we will only consider pressure gradients in the mean propagation direction x_1: only $F_1^v=F_v$ and $\Gamma_1=\Gamma$ may be non-zero. All pressure gradients are scaled by the pressure gradient inside the laminar flame zone:

$$\nabla P^*=\frac{\nabla P}{|\nabla P_{lam}|}\qquad\text{where}\qquad|\nabla P_{lam}|\simeq\rho_u(s_l^0)^2\tau/\delta_l^0 \tag{2.9}$$

where δ_l^0 is the unstrained laminar flame thickness which is obtained from the maximum temperature gradient $\delta_l^0=(T_b-T_u)/\mathrm{Max}(\mathrm{d}T/\mathrm{d}x)$ and ρ_u is the fresh gases density.

The pressure gradient ∇P_{lam} is created by dilatation inside the flame zone. It is large but, due to the thinnish flame front, the overall pressure jump ΔP between fresh and burnt gases remains small: $\Delta P/P\simeq\tau\gamma(s_l^0/a)^2$ where the ratio of flame to sound speeds, s_l^0/a, is of the order of 0.001. On the other hand, volume forces or external pressure gradients are imposed over distances much larger than the flamelet thickness and will overcome the effect of dilatation in turbulent flame brushes. These effects and their relative importance in various flames may be quantified in terms of two quantities: the reduced external pressure gradient ∇P_{ext}, and the reduced mean pressure gradient

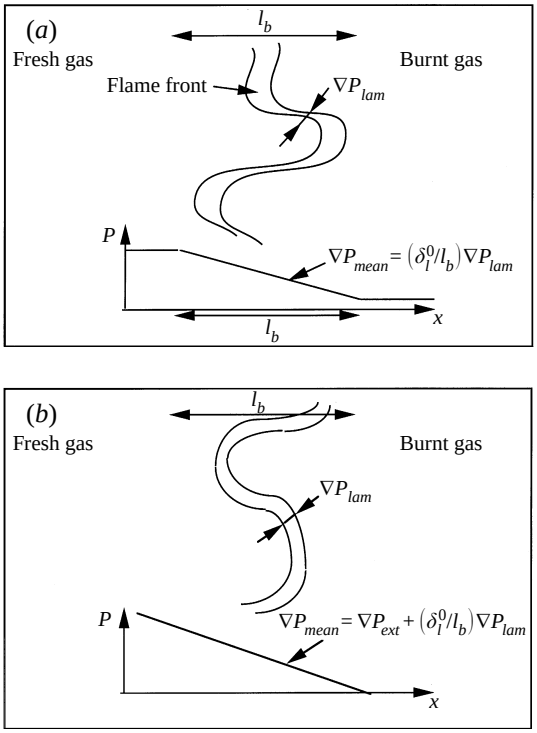

FIGURE 2. Pressure gradients in (*a*) a free flame ($\nabla P_{ext} = 0$); (*b*) a flame with imposed pressure gradient.

∇P_{mean}. We consider these gradients positive when the pressure increases when going from the fresh to the burnt gases. Figures 2(*a*) and 2(*b*) illustrate how these gradients may be estimated in a turbulent flame brush of thickness l_b with and without an external pressure gradient. With no external pressure gradient, corresponding to figure 2(*a*), the pressure jump across the flame will be slightly modified by flow divergence and spread over the flame brush thickness l_b so that the mean pressure gradient in the flame brush will be $\nabla P_{mean} \simeq \nabla P_{lam}\delta_l^0/l_b$. In the case of an externally imposed pressure gradient, corresponding to figure 2(*b*), ∇P_{mean} will be of the order of ∇P_{ext} everywhere in the flow: although the maximum instantaneous pressure gradient may still be found at the flame, ∇P_{ext} will be dominant over the flame brush thickness.

Pressure gradients in real flames are imposed either by flame confinement, as in ducted flows, or by gravity. Typical values of ∇P_{lam}, ∇P_{ext} and ∇P_{mean} are given in table 1 for different turbulent premixed flames along with their dimensional values. In the case of 'free' flames, the pressure gradient is imposed by the flame itself. The ducted flame data correspond to the experiment of Shepherd *et al.* (1982). The flame brush thickness is estimated by the integral length scale $l_t = 1$ cm.

These estimations indicate that the largest pressure gradients will be obtained in ducted flames. Gravity alone will create smaller effects. At this point, it is worth discussing the differences between flames subjected to a constant acceleration, such as gravity, or to a constant pressure gradient. In the first case, the induced pressure gradient is $\rho\Gamma$, which is different in the fresh and burnt gases, see below. For both cases, however, the pressure gradient will induce differential acceleration for fresh and burnt gas pockets thus leading to a modification of turbulent transport. Most

	s_l^0 (m s^{-1})	δ_l^0 (m)	T_b/T_u	$\lvert\nabla P_{lam}\rvert$ (Pa m^{-1})	$\lvert\nabla P_{ext}\rvert$ (Pa m^{-1})	$\lvert\nabla P_{ext}\rvert$	$\lvert\nabla P_{mean}\rvert$
Free flame	0.32	0.0005	6.5	1100	0	0	0.05
1 g flame	0.32	0.0005	6.5	1100	$\simeq 10$	0.009	0.059
Ducted flame	0.32	0.0005	6.5	1100	1000	0.91	0.96

TABLE 1. Typical pressure gradients for a propane/air flame ($P = 1$ atm, $\phi = 1.2$)

authors therefore expect similar effects from constant acceleration and from constant pressure gradients.

There are at least three ways to introduce pressure gradients in a direct numerical simulation of premixed turbulent flames: impose a constant volume force F_v; impose a pressure gradient through the boundary conditions; or impose a constant acceleration Γ, i.e. a volume force which is a function of the local density $F_g = \rho\Gamma$, where $\Gamma = g$ in the case of gravity. All techniques produce an imposed pressure gradient, see the Appendix. However, the first solution leads to a flow where the pressure gradient $\partial P/\partial x$ is compensated everywhere by the volume force F_v and has no effect on $\overline{\rho}\widetilde{u''c''}$. The second solution was investigated, but is difficult to implement in a simulation if the mean flow remains one-dimensional, which is required for statistical purposes. In this paper, we will use only the third solution with various values of the acceleration Γ.

3. Direct numerical simulation of premixed flames with pressure gradients

The present direct numerical simulations have been performed with a two-dimensional version of NTMIX. A complete description of this code may be found in Haworth & Poinsot (1992) or Poinsot & Lele (1992). It solves the fully compressible Navier–Stokes equations with a single finite-rate irreversible reaction $Fuel \rightarrow Products$. Variable density as well as viscosity and transport coefficients are taken into account. The conservation equations solved by the simulation are

$$\frac{\partial \rho}{\partial t} + \frac{\partial}{\partial x_i}(\rho u_i) = 0, \tag{3.1}$$

$$\frac{\partial \rho u_i}{\partial t} + \frac{\partial}{\partial x_j}(\rho u_i u_j) = -\frac{\partial p}{\partial x_i} + \rho\Gamma_i + \frac{\partial \tau_{ij}}{\partial x_j}, \tag{3.2}$$

$$\frac{\partial \rho E}{\partial t} + \frac{\partial}{\partial x_i}[(\rho E + p)u_i] = \rho\Gamma_i u_i + \frac{\partial}{\partial x_i}(u_j\tau_{ij}) + \frac{\partial}{\partial x_i}(\lambda\frac{\partial T}{\partial x_i}) + Q\dot{w}, \tag{3.3}$$

$$\frac{\partial(\rho\widetilde{Y})}{\partial t} + \frac{\partial}{\partial x_i}(\rho\widetilde{Y}u_i) = \frac{\partial}{\partial x_i}(\rho\mathscr{D}\frac{\partial \widetilde{Y}}{\partial x_i}) - \dot{w}, \tag{3.4}$$

where

$$\rho E = \frac{1}{2}\rho\sum_{k=1}^{3} u_k^2 + \frac{p}{\gamma - 1}, \tag{3.5}$$

$$\tau_{ij} = \mu\left(\frac{\partial u_i}{\partial x_j} + \frac{\partial u_j}{\partial x_i} - \frac{2}{3}\delta_{ij}\frac{\partial u_k}{\partial x_k}\right), \tag{3.6}$$

$$\dot{w} = \dot{w}_R/Y_R^o = \rho\widetilde{Y}B\exp\left(-\beta/\alpha\right)\exp\left(\frac{-\beta(1-\theta)}{1-\alpha(1-\theta)}\right). \tag{3.7}$$

$Re = aL_x/\nu$	L_e	Pr_o	T_a/T_b	T_b/T_u	b	s_l^0/a	δ_l^0/L_x	N_x
12000	1	0.75	8	4	0.76	0.0159	0.027	257

TABLE 2. Fixed parameters for direct numerical simulations of flames subjected to pressure gradients. The speed of sound and kinematic viscosity in the fresh gases are denoted by a and ν.

In these expressions ρ is the mass density, p is the thermodynamic pressure, ρE is the total energy density, and Q designates the heat of reaction per unit mass of fresh mixture ($Q = -\Delta h_f^o Y_R^o$ where Δh_f^o is the heat of reaction per unit mass of reactant). Γ_i are the i-component of the constant acceleration Γ. The reduced temperature is $\Theta = (T - T_u)/(T_b - T_u)$ where T_u is the fresh gas temperature and T_b is the adiabatic flame temperature. The activation temperature is T_a. B is the pre-exponential factor and the coefficients α and β are the temperature factor and the reduced activation energy, respectively,

$$\alpha = (T_b - T_u)/T_b; \qquad \beta = \alpha T_a/T_b. \tag{3.8}$$

The mass fraction of the reactants Y_R is non-dimensionalized by the initial mass fraction of reactants Y_R^o in the fresh gases: $\widetilde{Y} = Y_R/Y_R^o$. This varies from 1 in the fresh gases to 0 in the burnt gases.

We assume that the gas mixture is a perfect gas with constant molar mass and a specific heat ratio $\gamma = 1.4$. The thermal conductivity λ and the diffusion coefficient $\mathscr{D}$ are obtained from the viscosity coefficient μ according to

$$\lambda = \mu C_p/P_r \quad \text{and} \quad \mathscr{D} = \mu/(\rho S_c) \tag{3.9}$$

where the Prandtl number P_r and the Schmidt number S_c are constant. As a consequence the Lewis number $L_e = S_c/P_r$ is also constant. The viscosity μ is a function of temperature: $\mu = \mu_u(T/T_u)^b$.

The size of the computational domain is $L_x \times L_y$ with $N_x \times N_y$ grid points. In the present simulations, $N_x = 257$ and $N_y = 1025$. The aspect ratio of the box is $L_y/L_x = 6.66$. Run parameters are summarized in table 2.

4. Laminar flames subjected to pressure gradients

First, one-dimensional laminar flames are computed for $\tau = 3$ without and with an imposed constant acceleration Γ. Introducing the reduced acceleration, $g^* = \Gamma \delta_l^0/(s_l^0)^2$, which may be viewed as the inverse of a Froude number, four values of g^* are considered here: $g^* = 0$ (no imposed acceleration), $g^* = -6.25$ (favourable pressure gradient), $g^* = 3.12$ and $g^* = 6.25$ (adverse pressure gradient). Pressure profiles are plotted as a function of the downstream locations in figure 3(a) for the four g^* values. The pressure gradient $\nabla P = \rho\Gamma$ is $\rho_u(s_l^0)^2 g^*/\delta_l^0$ in the fresh gases and $\rho_b(s_l^0)^2 g^*/\delta_l^0$ in the burnt gases so that the reduced pressure gradient ∇P^* is g^*/τ in the fresh gases and $g^*/\tau(\tau+1)$ in the burnt gases. As expected, pressure gradients are constant for each side of the flame front but decrease by a factor $T_b/T_u = \tau + 1 = 4$ between fresh and burnt gases due to density changes. The pressure drop due to thermal expansion is apparent for the $g^* = 0$ case.

For all g^* values considered, the laminar flame structure is not affected by the imposed acceleration: flame thickness, reaction rate and mass fraction profiles remain unchanged. Nevertheless, due to the pressure gradient, a weak change in density,

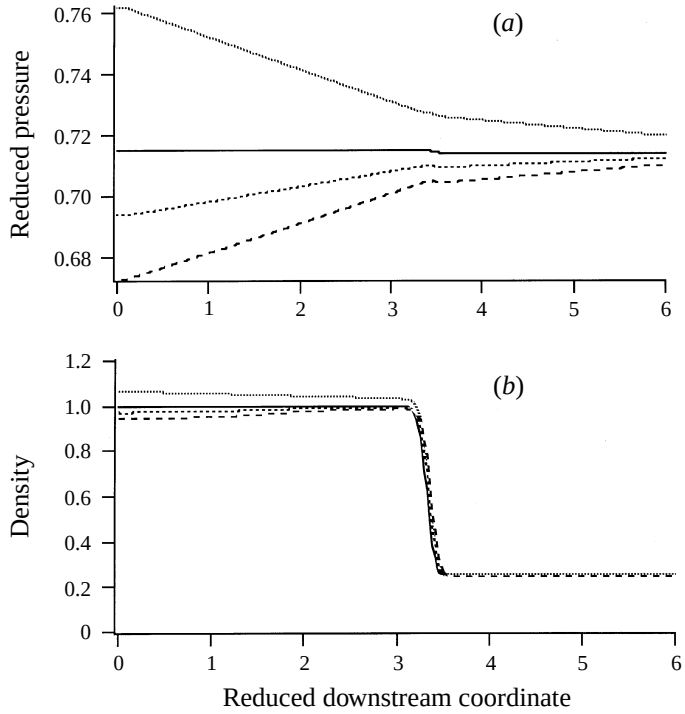

FIGURE 3. (*a*) Pressure and (*b*) density profiles in one-dimensional laminar flames without and with imposed acceleration g^* plotted as a function of the reduced downstream coordinate x/L_x. $g^* = 0$ (———); $g^* = -6.25$ (·····); $g^* = 3.12$ (– – –); $g^* = 6.25$ (— — —). In (*b*) the flame position corresponds to the change in the curve slopes.

similar to the one described in the Appendix, is observed inside the fresh or burnt gases, see figure 3(*b*), but remains negligible compared to the one induced by thermal expansion. The same trend is noticed for the flow velocity which is modified by about 3% by the pressure gradient and a factor of 4 by thermal expansion.

5. Turbulent flames subjected to pressure gradients

The previously computed one-dimensional laminar flames are used as initial solutions for two-dimensional flame-turbulence interaction simulations (figure 4). A Passot–Pouquet turbulence spectrum, with given turbulence intensity u' and integral length scale l_t, is superimposed on the combustion field (Haworth & Poinsot 1992). Two sets of numerical simulations have been conducted. The first set (runs A–C) starts from a high turbulence level ($u'_0/s^0_l = 5$) and a zero pressure gradient ($g^* = 0$) case (run A). This flame exhibits gradient transport as expected by the value of the number $N_B = 0.6$ (equation (1.3)). A favourable pressure gradient (i.e. $g^* < 0$) is then imposed for runs B and C to reach a counter-gradient diffusion situation. The second set (runs D–F) starts from a low turbulence level ($u'_0/s^0_l = 2$) with a zero pressure gradient case (run D) which corresponds to a counter-gradient situation, with an initial number $N_B = 1.5$. Under an adverse pressure gradient (i.e. $g^* > 0$), the flow is found to exhibit gradient turbulent transport for runs E and F. Numerical parameters are displayed on table 3 where g^* is the reduced imposed acceleration ($g^* = \Gamma\,\delta^0_l/(s^0_l)^2$).

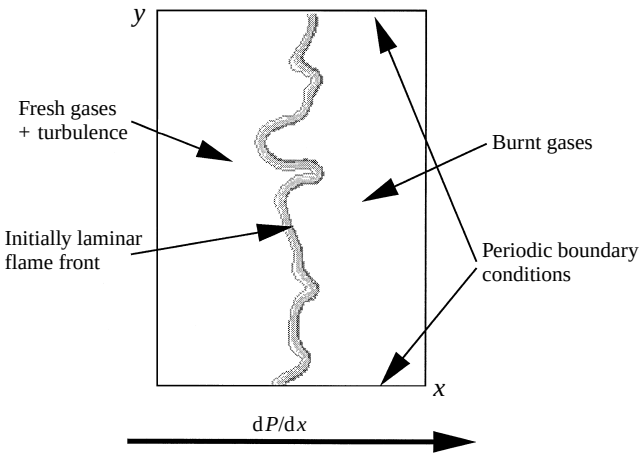

FIGURE 4. Configuration for the numerical simulations.

Case	u'_0/s^0_l	l_t/δ^0_l	g^*	N_x	N_y
A	5	3.5	0	257	1025
B	5	3.5	−3.12	257	1025
C	5	3.5	−6.25	257	1025
D	2	3.5	0	257	1025
E	2	3.5	3.12	257	1025
F	2	3.5	6.25	257	1025

TABLE 3. Numerical parameters for direct numerical simulations of two-dimensional turbulent flames

The values of ∇P_{mean} were chosen of the order of the pressure gradient found in the experiment of Shepherd *et al.* (1982).

Since we will use a BML formulation to analyse DNS results and the BML theory uses a flamelet assumption, it is useful to described the regime of combustion for the DNS of table 3. In a Borghi–Barrère diagram, these regimes are slightly above the Klimov–Williams limit but well below the limit proposed by Poinsot, Veynante & Candel (1991) suggesting that they satisfy the flamelet assumption. DNS confirm that all flame fronts in table 3 remain 'flamelet-like': the front is thin and connected, no quenching takes place and flamelet concepts may be used to analyse data.

An additional point is related to two-dimensional versus three-dimensional DNS. A comparison (Veynante *et al.* 1997) shows that similar conclusions are obtained when considering turbulent diffusion fluxes (i.e. the occurrence of counter-gradient diffusion). However, since two-dimensional DNS allow a much larger range of parameters to be investigated, it was used for the present work.

5.1. *Effect of the mean pressure gradient on the turbulent flame structure*

Instantaneous temperature and vorticity fields are displayed in figure 5(*a*) for an initial turbulence level $u'_0/s^0_l = 5$ without (case A) and with (case C) an imposed mean pressure gradient. Corresponding pressure fields are displayed in figure 5(*b*). The flame structures are quite different. Owing to the favourable pressure gradient ($\partial\overline{P}/\partial x < 0$), the wrinkling of the flame front is less and the turbulent flame brush is

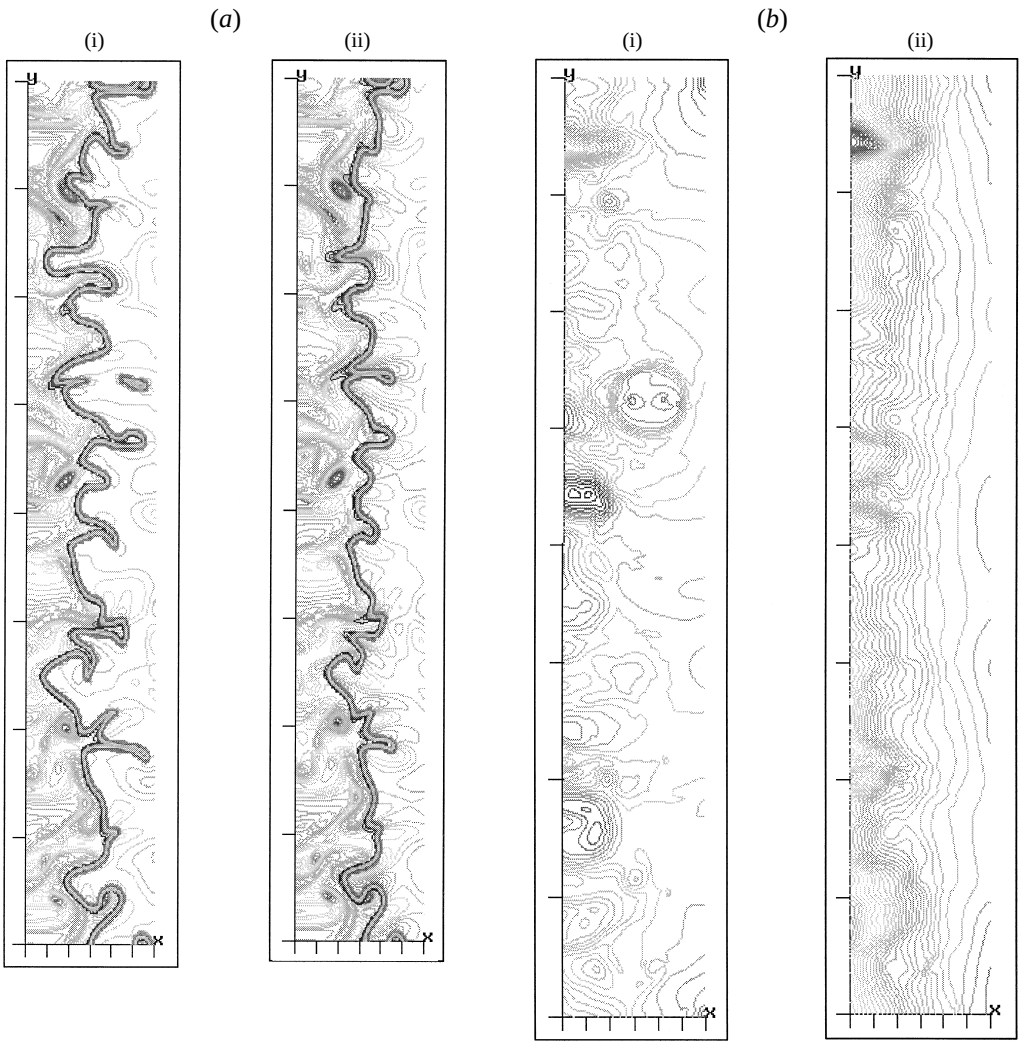

FIGURE 5. (*a*) Superimposed instantaneous temperature and vorticity fields at time $t = 2.7\delta_l^0/s_l^0$. Initial turbulence level $u_0'/s_l^0 = 5$. (i) No imposed pressure gradient ($g^* = 0$. – case A); (*b*) favourable imposed pressure gradient ($g^* = -6.25$ – case C). $0 \leqslant (T - T_u)/(T_b - T_u) \leqslant 1$ and $-6.2 \leqslant \omega\delta_l^0/s_l^0 \leqslant 6.8$. The temperature T is reduced using the fresh (T_u) and the burnt (T_b) gases temperatures. The vorticity ω is reduced with the laminar flame time δ_l^0/s_l^0. (*b*) As (*a*) but for the instantaneous pressure field (i) $0.70 \leqslant P/(\rho_u a^2) \leqslant 0.76$; (ii) $0.71 \leqslant P/(\rho_u a^2) \leqslant 0.79$. The pressure P is reduced using the unburnt gases density ρ_u and the sound speed a.

thinner. Despite similar minimum and maximum values, the pressure field is mainly dominated by vortices in case A whereas the pressure gradient, imposed by the constant acceleration Γ, is clearly apparent for case C.

Close-up views of the temperature and vorticity fields of figure 5(*a*) are displayed in figure 6. As previously described, the flame front is less wrinkled in case C despite a similar turbulence distribution in the fresh gases.

Instantaneous temperature and vorticity fields are displayed for cases D and F in figure 7. The initial turbulence level is lower ($u_0'/s_l^0 = 2$): without an externally imposed pressure gradient, this flow exhibits a counter-gradient turbulent transport as

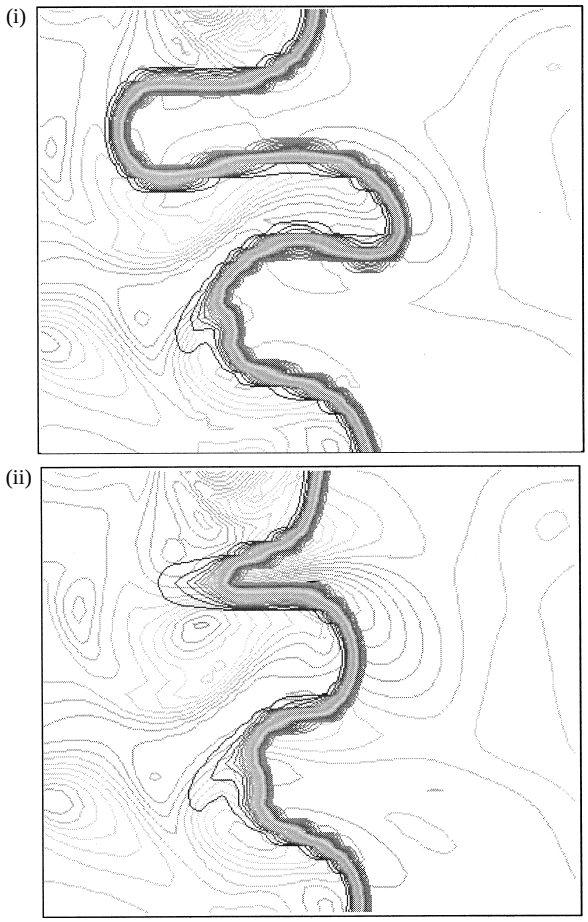

FIGURE 6. Superimposed instantaneous temperature and vorticity fields at time $t = 2.7\delta_l^0/s_l^0$. Zoom from figure 5(*a*). Initial turbulence level $u_0'/s_l^0 = 5$. (i) No imposed pressure gradient ($g^* = 0$ – case A); (ii) favourable imposed pressure gradient ($g^* = -6.25$ – case C).

predicted by the criterion of equation (1.3): $N_B = 1.5$. In case F, an adverse pressure gradient is imposed and a transition towards gradient transport is expected. The flame front wrinkling is also somewhat increased by the adverse pressure gradient, due to the differential acceleration induced by buoyancy between fresh and burnt gases.

5.2. *Effect of the mean pressure gradient on global turbulent flame characteristics*

The global turbulent flame characteristics, namely the turbulent flame speed S_T and flame brush thickness δ_T, are plotted in figures 8 and 9 as a function of reduced time (t/t_F where $t_F = \delta_l^0/s_L^0$) for different values of g^*. As expected from the previous flow-field visualizations, a favourable pressure gradient, i.e. $\partial\overline{P}/\partial x < 0$, which is generally encountered in practical situations of confined turbulent flames, leads to a thinner turbulent flame brush and a lower turbulent flame speed. The decrease in S_T may reach 30%. On the other hand, an adverse pressure gradient, i.e. $\partial\overline{P}/\partial x > 0$, induces an increase in flame brush thickness and a higher turbulent flame speed.

From theoretical analysis, Libby (1989) has shown that, under steady-state conditions, a constant acceleration Γ adds a linear buoyancy term to the turbulent flame

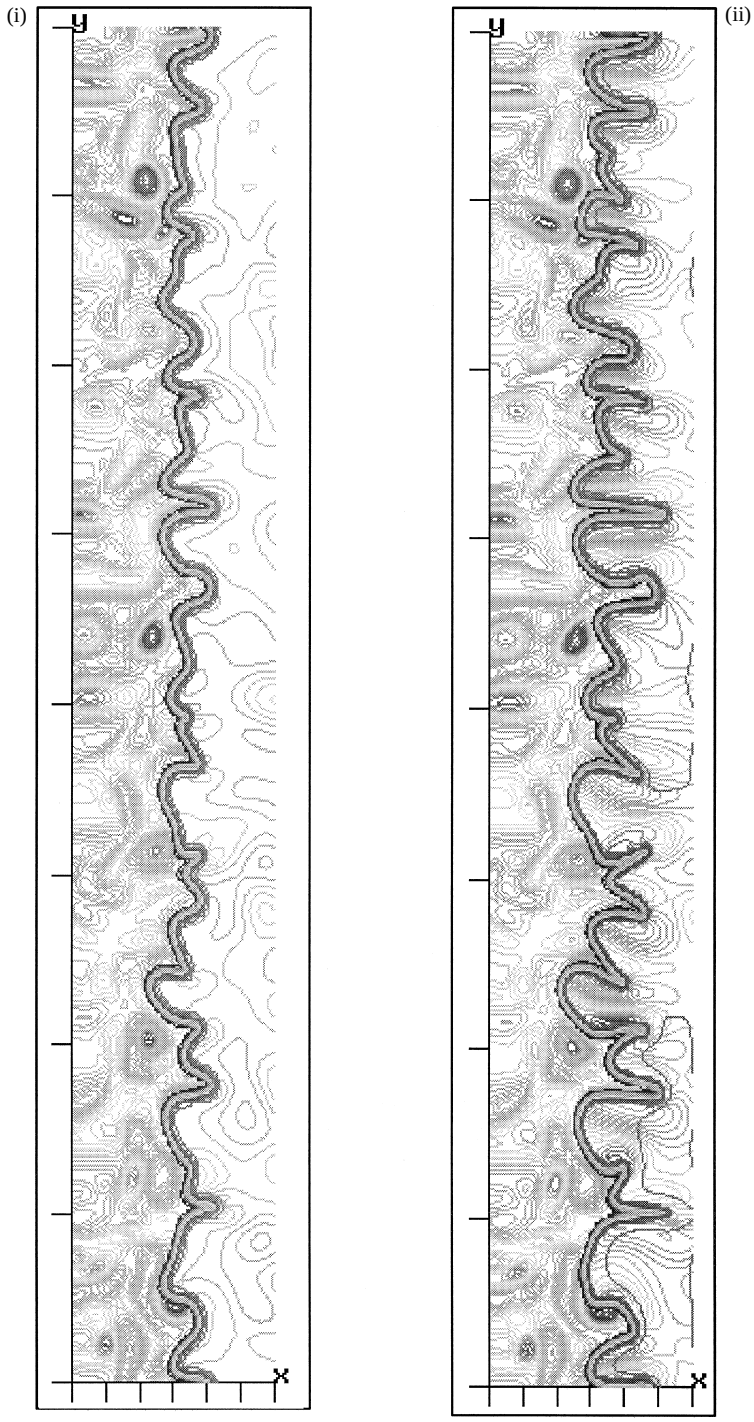

FIGURE 7. Superimposed instantaneous temperature and vorticity fields at time $t = 2.7\delta_l^0/s_l^0$. Initial turbulence level $u_0'/s_l^0 = 2$. (i) No imposed pressure gradient ($g^* = 0$ – case D); (ii) adverse imposed pressure gradient ($g^* = 6.25$ – case F). $0 \leqslant (T - T_u)/(T_b - T_u) \leqslant 1$ and $-2.6 \leqslant \omega\delta_l^0/s_l^0 \leqslant 2.8$. The temperature T is reduced using the fresh (T_u) and the burnt (T_b) gases temperatures. The vorticity ω is reduced with the laminar flame time δ_l^0/s_l^0.

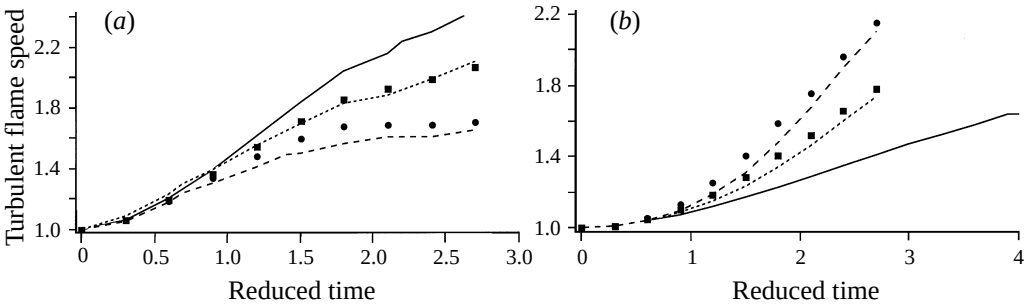

FIGURE 8. Reduced turbulent flame speed S_T/s_l^0 plotted as a function of the reduced time $t/t_f = s_l^0 t/\delta_l^0$, where $t_f = \delta_l^0/s_l^0$ is a flame time, for different values of g^*. (*a*) Initial turbulent level $u_0'/s_l^0 = 5$: cases A (———), B (·····) and C (– – – –); (*b*) initial turbulent level $u_0'/s_l^0 = 2$: cases D (———), E (·····) and F (– – – –); symbols correspond to estimates from Libby theory: (*a*) cases B (■) and C (●); (*b*) cases E (■) and F (●).

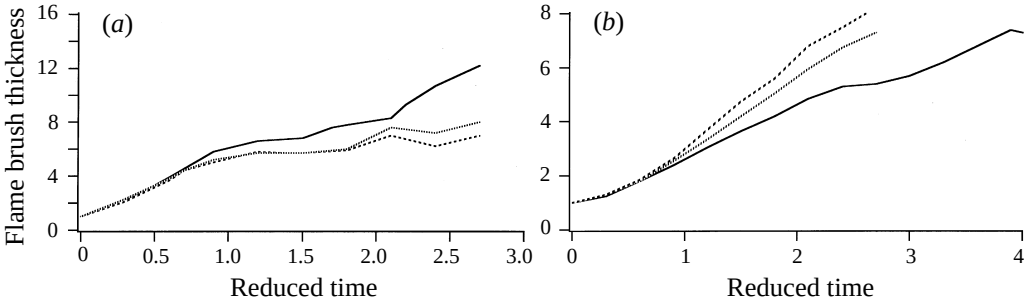

FIGURE 9. As figure 8 but for reduced turbulent flame thickness δ_T/δ_l^0. The turbulent flame brush is determined from the maximum value of the $\tilde{c}$ gradient ($\delta_t = 1/\mathrm{Max}\left(\partial\tilde{c}/\partial x\right)$)

speed S_T:

$$\frac{S_T}{u_0'} = \frac{2}{(1+\lambda)^{1/2}} + \frac{\tau}{(1+\tau)(1+\lambda)}\frac{\Gamma l_t}{s_l^0 u_0'} \tag{5.1}$$

where τ is the heat release factor and λ an empirical constant chosen to be $\lambda = 0.017$. This expression may be recast as

$$S_T(g^*) = S_T(g^* = 0) + \beta g^* s_l^0 \frac{l_t}{\delta_l^0} \tag{5.2}$$

where $S_T(g^* = 0)$ is the turbulent speed of a free flame (with no imposed pressure gradient) and $\beta = \tau/(1+\tau)(1+\lambda)$ a constant.

In the present DNS, unsteady effects are important and Libby's analysis may be extended using a variable β. The function β depends on time and is estimated as the averaged value of β^{AC} and β^{DF} respectively computed from cases A and C and cases D and F as

$$\beta(t) = \frac{\beta^{AC}(t) + \beta^{DF}(t)}{2} \tag{5.3}$$

$$\text{with} \quad \beta^{AC}(t) = \frac{S_T^C(t) - S_T^A(t)}{g_C^* s_l^0 l_t/\delta_l^0}$$

$$\text{and} \quad \beta^{DF}(t) = \frac{S_T^F(t) - S_T^D(t)}{g_F^* s_l^0 l_t/\delta_l^0}$$

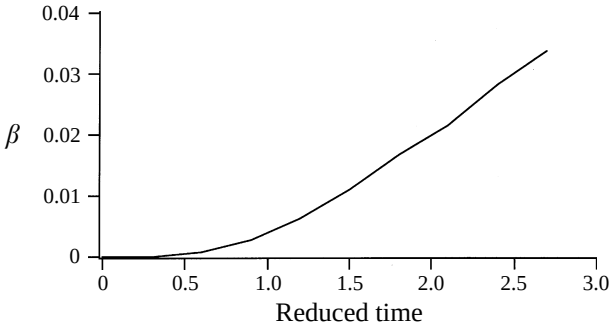

FIGURE 10. The function β, defined by expression (5.4), is plotted versus the reduced time t.

where S_T^X denotes the turbulent flame speed in case X, $g_C^* = -6.25$ and $g_F^* = 6.25$. The laminar flame speed s_l^0 and the length-scale ratio l_t/δ_l^0 are identical for all cases and given in table 3. The function $\beta(t)$ is plotted on figure 10. Then, extending the theory developed by Libby (1989), the turbulent flame speed may be estimated as

$$S_T\left(g^*, l_t, t\right) = S_T\left(g^* = 0, l_t, t\right) + \beta(t) s_l^0 g^* \frac{l_t}{\delta_l}. \tag{5.4}$$

Expression (5.4) is used to evaluate turbulent flame speed for cases B, C, E and F. The agreement with DNS data is very good as shown on figure 8, corresponding to the Libby theory, even under non-steady conditions. Accordingly, a constant acceleration Γ tends to modify the turbulent flame speed by adding a linear buoyancy term proportional to the product $g^* l_t$.

One may note that, according to Libby's theory (equation (5.1)), the value of the constant β should be 0.74 ($\tau = 3$ and $\lambda = 0.017$). Figure 10 displays values about 25 times lower. This discrepancy may be explained by the unsteady effects in our simulations. As shown in figure 10, $\beta(t)$ does not reach a steady value whereas Libby's theory assumes constant turbulence characteristics. Following Libby, the turbulent flame speed without imposed constant acceleration is given by (5.1):

$$\frac{S_T}{s_l^0} = \frac{2}{(1+\lambda)^{1/2}} \frac{u_0'}{s_l^0}, \tag{5.5}$$

leading to reduced turbulent flame speeds $S_T/s_l^0 = 9.9$ for case A and $S_T/s_l^0 = 5.9$ for case D, values higher than the ones displayed on figure 8. On the other hand, estimating the empirical constant λ from (5.5) and DNS-extracted values of the turbulent flame speed S_T leads to $\lambda \approx 25$ corresponding to a value of β about 25 times lower that the value predicted by Libby's theory and in agreement with our numerical data.

5.3. *Turbulent transport* $\widetilde{\overline{\rho} u'' c''}$

The transverse profiles of the turbulent flux $\widetilde{\overline{\rho} u'' c''}$ as a function of the mean progress variable $\widetilde{c}$ for cases A and C at various times are shown in figure 11. Case A, without an imposed mean pressure gradient, is clearly of gradient type, i.e. $\widetilde{\overline{\rho} u'' c''} < 0$, whereas the imposed favourable pressure gradient leads to a counter-gradient turbulent transport. This finding is in agreement with the work of Bray *et al.* (1982) and is expected from

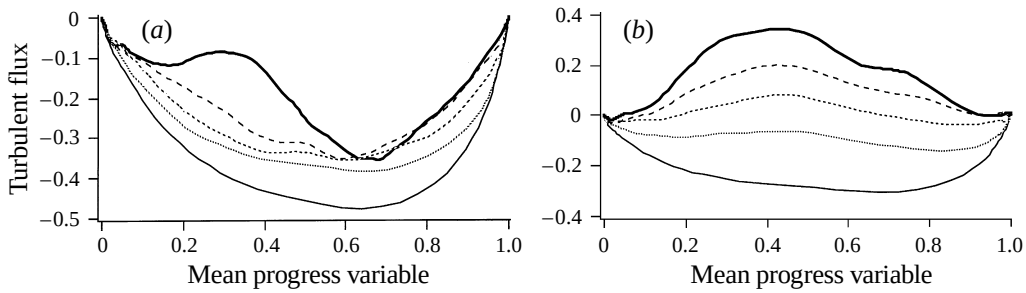

FIGURE 11. Transverse profiles of the turbulent flux $\overline{\rho}\widetilde{u_1''c''}$ plotted as a function of the mean progress variable $\widetilde{c}$ for different reduced time steps $t^+ = t/t_f$ where $t_f = \delta_l^0/s_l^0$ is a flame time. Initial turbulence level $u_0'/s_l^0 = 5$. $t^+ = 0.6$ (———); 0.9 (·····); 1.2 (– – – –); 1.5 (— — —); 1.8 (——). (*a*) No imposed pressure gradient ($g^* = 0$ – case A); (*b*) favourable imposed pressure gradient ($g^* = -6.25$ – case C). Turbulent fluxes are non-dimensionalized by $\rho_u s_l^0$.

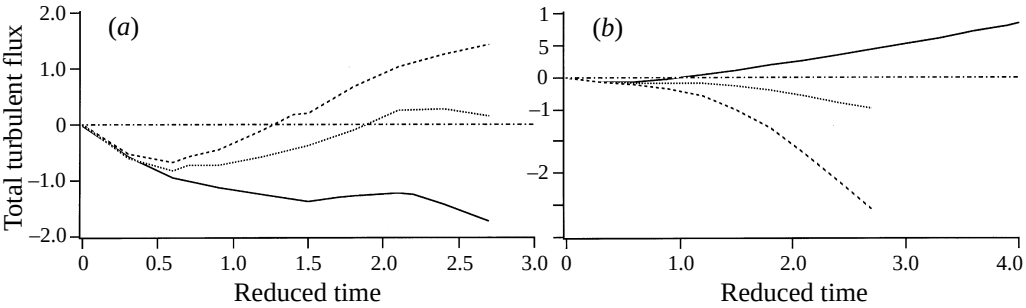

FIGURE 12. Total turbulent flux $\int_{-\infty}^{+\infty} \overline{\rho}\widetilde{u_1''c''}\mathrm{d}x$ plotted as a function of the reduced time t/t_f where $t_f = \delta_l^0/s_l^0$ is a flame time. (*a*) Initial turbulence level $u_0'/s_l^0 = 5$: cases A (———), B (·····) and C (– – – –); (*b*) initial turbulence level $u_0'/s_l^0 = 2$: cases D (———), E (·····) and F (– – – –). Total turbulent fluxes are non-dimensionalized by $\rho_u s_l^0 \delta_l^0$.

(2.4). Even in clearly counter-gradient situations, the turbulent flux $\overline{\rho}\widetilde{u''c''}$ is always negative, or of gradient type, at the leading edge of the flame brush, where $\widetilde{c} \to 0$. As shown by Bray and his coworkers, these gradient zones allow flame stabilization.

The total turbulent flux, i.e. $\int_{-\infty}^{+\infty} \overline{\rho}\widetilde{u_1''c''}\mathrm{d}x$, is plotted as a function of the reduced time for the different simulations in figure 12. Favourable pressure gradients promote counter-gradient diffusion and a reduction of both the turbulent flame speed S_T and the turbulent flame thickness δ_T. On the other hand, adverse pressure gradients lead to an increase in S_T and δ_T and induce gradient turbulent transport.

5.4. *Analysis of the $\overline{\rho}\widetilde{u''c''}$ transport equation*

All terms in the transport equation for $\overline{\rho}\widetilde{u''c''}$, (2.4), may be obtained from direct numerical simulations. A typical DNS evaluation of terms (I)–(X) appearing in the $\widetilde{c}$-flux budget of (2.4) is presented in figure 13(*a*) for case D. The figure also displays the imbalance (i.e. the difference between the sums of the right- and left-hand-side terms) that was found when numerically closing the $\widetilde{c}$-flux budget in (2.4). This imbalance is due to inherent numerical errors involved in the simulations as well as in the post-processing of the data. Its magnitude remains small (less than 3% of the maximum term), which suggests that the simulations can be used to analyse the variations of

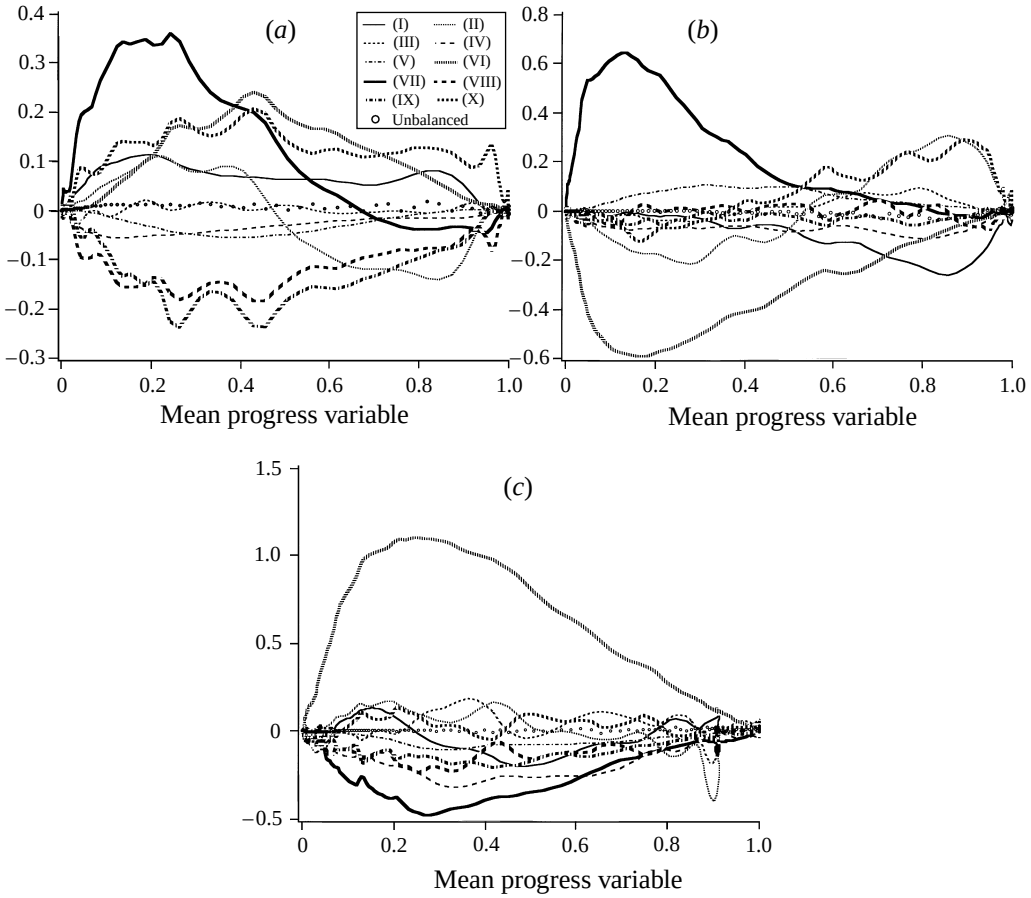

FIGURE 13. Variations of the different terms appearing in the $\widetilde{c}$-flux budget (equation. (2.4)) across the turbulent flame brush. (*a*) Case D: counter-gradient turbulent diffusion and no imposed pressure gradient. Reduced time is $ts_l^0/\delta_l^0 = 2.1$. (*b*) Case F: gradient turbulent diffusion induced by an adverse mean pressure gradient. Reduced time $ts_l^0/\delta_l^0 = 2.1$. (*c*) Case C: counter-gradient turbulent diffusion induced by a favourable mean pressure gradient. Reduced time is $ts_l^0/\delta_l^0 = 2.7$. Terms are non-dimensionalized by $\rho_u \left(s_l^0\right)^2/\delta_l^0$.

second-order moments. For instance, figure 13(*a*) shows that the dissipation terms (VIII) and (IX), which are generally modelled together, are of the same order and act to promote gradient diffusion. On the other hand, pressure terms (VI) and (VII), and the velocity–reaction rate correlation (X), strongly act to promote counter-gradient diffusion. The two source terms due to mean progress variable gradient (IV) and mean velocity gradient (V) tend to decrease the turbulent fluxes as expected and accordingly, in the present counter-gradient situation, act to promote gradient turbulent diffusion. The mean pressure gradient term (term VI) corresponds to the pressure jump across the flame brush (see figure 14):

$$-\overline{c''}\frac{\partial \overline{p}}{\partial x} = -(\overline{c} - \widetilde{c})\frac{\partial \overline{p}}{\partial x} \approx \tau \frac{\widetilde{c}(1-\widetilde{c})}{1+\tau\widetilde{c}} \frac{\rho_u \tau (s_l^0)^2}{\delta_T}. \tag{5.6}$$

The fluctuating pressure term (VII) cannot be neglected as generally assumed in the models proposed to close the transport equation (2.4).

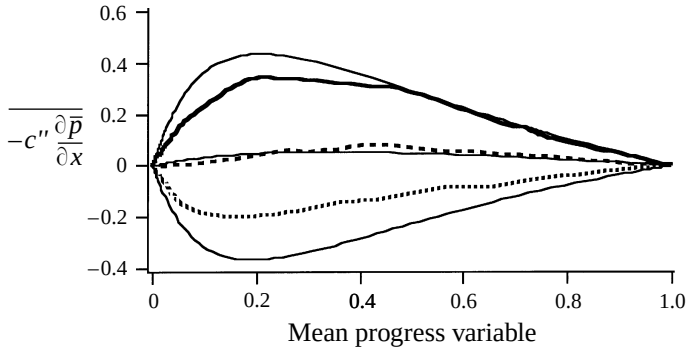

FIGURE 14. Comparison between direct numerical simulation data for cases C (———), D (– – – –) and F (·····) and modelled mean pressure gradient source term (———) from (5.7) in the the $\widetilde{c}$-flux transport equation (2.4). Pressure gradients are non-dimensionalized by $\rho_u \tau \left(s_l^0\right)^2 / \delta_l^0$. Reduced time is $ts_l^0/\delta_l^0 = 2.1$.

A similar analysis is now performed for case F, where, due to the imposed adverse pressure gradient, the turbulent diffusion becomes of gradient type, as indicated in figure 13(*b*). As expected, the mean pressure gradient term tends to promote gradient turbulent diffusion and corresponds to the imposed pressure gradient. Once again, the fluctuating pressure term (VII) is not negligible and acts to counterbalance the mean pressure gradient term (VI). In fact, the combined term (VI) + (VII) is mainly negative and corresponds to a gradient diffusion. The reaction term acts to promote counter-gradient diffusion.

The budget of the transport equation for $\overline{\rho}\widetilde{u_1''c''}$ for case C is presented in figure 13(*c*). The favourable mean pressure gradient acts to promote counter-gradient turbulent diffusion from term (VI). Once again, term (VII) tends to counterbalance term (VI). For such a situation, Bray *et al.* (1982) and Libby (1989) propose neglecting the pressure fluctuation effects (term VII). Bray *et al.* (1982) assume that only the cross-dissipation terms (VIII + IX) can provide a balance for the mean pressure term (VI). In fact, from our simulation, the mean pressure term (VI) is balanced by the sum of the three contributions: the cross-dissipation term (VIII + IX), the pressure fluctuation term (VII) that cannot be neglected, and the source term due to gradients of $\widetilde{c}$ (IV).

The mean pressure gradient across the flame brush may be simply modelled as the sum of two contributions: the imposed pressure gradient, and the pressure jump due to thermal heat release. As a result, the source term (VI) in $\rho\widetilde{u''c''}$ becomes

$$-\overline{c''\frac{\partial \overline{p}}{\partial x}} = -(\overline{c}-\widetilde{c})\frac{\partial \overline{p}}{\partial x} \approx \tau \frac{\widetilde{c}(1-\widetilde{c})}{1+\tau\widetilde{c}}\left[\frac{\rho_u \tau (s_l^0)^2}{\delta_T} - \overline{\rho}\Gamma\right] \tag{5.7}$$

where $\overline{\rho}\Gamma$ corresponds to the imposed pressure gradient. This expression is verified in the present simulations (figure 14).

As pointed out, the fluctuating pressure term (VII) in (2.4) acts to counterbalance the mean pressure gradient term (VI) for cases C and F and is of the same order of magnitude. This quite surprising result may be easily explained as follows. Neglecting the pressure jump at the flame front and assuming that the instantaneous local pressure gradient is given by

$$\frac{\partial p}{\partial x} = \rho\Gamma \tag{5.8}$$

leads to the following estimates for terms (VI) and (VII) in (2.4):

$$-\overline{c''}\frac{\partial \overline{p}}{\partial x} \approx -\overline{\rho}\,\overline{c''}\Gamma, \tag{5.9}$$

$$-\overline{c''\frac{\partial p'}{\partial x}} \approx -\overline{\rho' c''}\Gamma. \tag{5.10}$$

As $\overline{c''}$ is always positive (see (2.5)), the sign of the mean pressure term (VI) is opposite to the sign of the imposed acceleration Γ. On the other hand, when c increases ($c'' \geqslant 0$), the density ρ decreases ($\rho' \leqslant 0$). Accordingly, $\overline{\rho' c''}$ is negative and the fluctuating pressure term (VII) has the same sign as the acceleration Γ. Pressure terms (VI) and (VII) in the balance equation for the turbulent fluxes $\widetilde{\overline{\rho} u'' c''}$ act in an opposite way with a sign depending on Γ. Obviously, there are limits to this qualitative approach and the estimates of (5.9) and (5.10) are too crude, leading to a zero total contribution of terms (VI) and (VII) ($\overline{\rho}\,\overline{c''}\Gamma + \overline{\rho' c''}\Gamma = \overline{\rho c''}\Gamma = 0$) that is not observed in DNS data. However two main conclusions arise from this finding. First, the fact that the fluctuating pressure term (VII) tends to counterbalance the mean pressure term (VI) is due to the use of a constant acceleration Γ and should not be observed for a constant pressure gradient. Second, terms (VI) and (VII) are strongly coupled and have to be modelled together as $\overline{c''\partial p/\partial x}$. The modelling of term (VI+VII) will be discussed later with reference to DNS data (§6.3).

6. Theoretical analysis and modelling

6.1. *Model for turbulent flux without pressure gradient*

In this section, we first recall the derivation of a model for the turbulent flux of the mean progress variable $\widetilde{c}$. Details may be found in Veynante *et al.* (1997). This derivation starts from a relation proposed by Bidaux & Bray (1994, unpublished) expressing the flame-front averaged velocity, $\langle u_i \rangle_s$ as a weighted average of the mean unburnt and burnt gases conditional velocities:

$$\langle u_i \rangle_s = (1-K)\,\overline{u}_{iu} + K\,\overline{u}_{ib} \tag{6.1}$$

where K is a constant ($0 \leqslant K \leqslant 1$) related to the iso-$c$ level used to defined the flame location. This expression assumes a linear variation of the mean flow velocity across the flame. Furthermore, using the classical BML framework, we can easily relate unconditional to conditional statistics:

$$\widetilde{u}_i = (1-\widetilde{c})\overline{u}_{iu} + \widetilde{c}\overline{u}_{ib}. \tag{6.2}$$

Equations (6.1) and (6.2) lead to

$$\langle u_i'' \rangle_s = \langle u_i \rangle_s - \widetilde{u} = (K-\widetilde{c})\,(\overline{u}_{ib} - \overline{u}_{iu}). \tag{6.3}$$

From (2.1), the previous relation leads to

$$\langle u_i'' \rangle_s = \frac{(K-\widetilde{c})}{\widetilde{c}\,(1-\widetilde{c})}\widetilde{u_i'' c''}. \tag{6.4}$$

Thus, the turbulent diffusion velocity, $\langle u_i'' \rangle_s$, is simply related to the turbulent flux of $\widetilde{c}$. This expression is used by Bidaux & Bray (1994, unpublished) to relate the turbulent flux of flame surface density Σ, $\langle u_i'' \rangle_s \Sigma$, to the turbulent flux of mean progress variable $\widetilde{c}$. This expression may be used to derive an estimate of $\widetilde{u_i'' c''}$ via a model for the mean velocity fluctuation $\langle u_i'' \rangle_s$: considering limiting cases of low turbulence levels, where

flow dynamics is mainly controlled by thermal expansion across the flame brush, and high turbulence levels, where the turbulent velocities dominate the flow induced by thermal expansion, Veynante *et al.* (1997) proposed the following expression for $\langle u_1'' \rangle_s$ where index 1 corresponds to the direction normal to the flame:

$$\langle u_1'' \rangle_s = (K - \widetilde{c})\left(\tau s_l^0 - 2\alpha u'\right), \tag{6.5}$$

leading to

$$\widetilde{u_1'' c''} = \widetilde{c}\,(1 - \widetilde{c})\left(\tau s_l^0 - 2\alpha u'\right) \tag{6.6}$$

and to the criterion (1.3). Here u' denotes the r.m.s. velocity fluctuations and α is an efficiency function to take into account the low ability of small turbulent vortices to affect the flame front. The function α, depending on the length-scale ratio l_t/δ_l^0, may be found in Veynante *et al.* (1997) or on figure 1. In the present simulations, $\alpha \approx 0.5$

6.2. *Model for turbulent flux with pressure gradient*

Our objective in this section is to incorporate pressure gradient effects in the previous analysis. Pressure gradients induce differential buoyancy effects between cold heavy reactants and light hot products. We quantify this buoyancy effect through a characteristic velocity $U_B(\widetilde{c})$ which is simply added to the two velocities used in (6.5): the velocity induced by the flame, $(K - \widetilde{c})\tau s_l^0$; and the velocity induced by turbulence, $2(K - \widetilde{c})\alpha u'$,

$$\langle u_1'' \rangle_s = (K - \widetilde{c})\left(\tau s_l^0 - 2\alpha u'\right) + U_B(\widetilde{c}). \tag{6.7}$$

The estimation of $U_B(\widetilde{c})$ is done as follows. In the fresh gases, $U_B(0) = U_B^b$ corresponds to the relative speed of a pocket of burnt gas (density ρ_b, diameter l). Similarly a velocity $U_B(1) = U_B^u$ will be associated with the movement of unburnt gas pockets in the burnt products. Assuming an equilibrium between buoyancy and drag forces (Batchelor 1967), U_B^b is determined from

$$\tfrac{1}{2}\rho_u C_x S \left(U_B^b\right)^2 = (\rho_b - \rho_u)\, V \Gamma \tag{6.8}$$

where V is the volume of the pocket of burnt gases in the fresh gases. S corresponds to the projected surface of the pocket on a plane normal to the velocity direction. Following the Stokes law, the drag coefficient C_x is given by

$$C_x = \frac{24}{Re} = \frac{24}{U_B^b l/\nu} \tag{6.9}$$

where ν is the dynamic viscosity in the fresh gases and l a characteristic length scale of the pocket of burnt gases. Then

$$U_B^b = \frac{1}{12\nu}\frac{\rho_b - \rho_u}{\rho_u}\frac{Vl}{S}\Gamma = -\frac{1}{12\nu}\frac{\tau}{\tau + 1}\frac{Vl}{S}\Gamma. \tag{6.10}$$

For a pocket of fresh gases with density ρ_u and diameter l embedded in burnt gases the same analysis leads to a relative displacement speed U_B^u:

$$U_B^u = \frac{1}{12\nu_b}\frac{\rho_u - \rho_b}{\rho_b}\frac{Vl}{S}\Gamma = \frac{1}{12\nu_b}\tau\frac{Vl}{S}\Gamma \tag{6.11}$$

where ν_b is the kinematic viscosity in the burnt gases.

Assuming a linear variation of the buoyancy velocity $U_B(\widetilde{c})$ with $\widetilde{c}$ between the

flame leading and trailing edges leads to

$$U_B(\widetilde{c}) \approx \frac{1}{12 v_u} \frac{\tau}{\tau+1} \frac{Vl}{S} \Gamma \left[\left(1+(\tau+1)^{1-n}\right) \widetilde{c} - 1 \right] \tag{6.12}$$

where the kinematic viscosity ratio has been estimated as

$$\frac{v_u}{v_b} \approx \left(\frac{T_u}{T_b}\right)^n = \left(\frac{1}{\tau+1}\right)^n \tag{6.13}$$

with $n = 1.76$.

For $3 \leqslant \tau \leqslant 6$, we have $0.74 \leqslant 1/\left(1+(\tau+1)^{1-n}\right) \leqslant 0.8$ which is of the order of magnitude of the constant K. In a first step, equation (6.12) is simply rewritten: $K = 1/\left(1+(\tau+1)^{1-n}\right)$, leading to

$$U_B(\widetilde{c}) \approx \frac{1}{12 v_u} \frac{\tau}{K\,(\tau+1)} \frac{Vl}{S} \Gamma\,(\widetilde{c} - K), \tag{6.14}$$

which may be rewritten as

$$U_B(\widetilde{c}) \approx \frac{Re_f}{12K} \frac{\tau}{\tau+1} \frac{Vl}{S\left(\delta_l^0\right)^2} s_l^0 g^*\,(\widetilde{c} - K) \tag{6.15}$$

where $Re_f = \delta_l^0 s_l^0 / v_u$ is a flame Reynolds number.

Two comments arise from this result.

First, the non-dimensionalized ratio $Vl/S\left(\delta_l^0\right)^2$ may be viewed as a form factor of the gas pocket of size l. In a first step, this ratio may be assumed to be proportional to $\left(l_t/\delta_l^0\right)^2$ where l_t is the integral length scale, a rough estimate of the flame front wrinkling scale. In our simulations, the ratio $\left(l_t/\delta_l^0\right)^2$ is kept constant. Nevertheless, the dependence of the buoyancy velocity U_B on the integral length scale l_t remains an open question which is difficult to investigate using DNS because the simulations are limited to a weak range of the ratio l_t/δ_l^0. One may expect that for large values of the integral length scale l_t, the wrinkling of the flame front remains quite low. Accordingly, the assumption of a pocket of fresh (respectively burnt) gases in burnt (fresh) gases is probably not valid and expression (6.15) overestimates the buoyancy-induced velocity.

In the case of a sphere of fluid 1 moving freely under gravity in a fluid 2, Batchelor proposes a correction factor C to the velocity induced by buoyancy:

$$C = \frac{\mu_2 + \mu_1}{\mu_2 + \frac{3}{2}\mu_1} \tag{6.16}$$

where μ_1 and μ_2 denotes the dynamic viscosities of fluid 1 and 2 respectively. This correction is neglected here and is incorporated in K and the modelling constant a.

Then, from (6.4) and (6.7), a simple model for the turbulent flux $\widetilde{u_1'' c''}$ is

$$\widetilde{u_1'' c''} = \widetilde{c}(1-\widetilde{c}) \left(\tau s_l^0 - 2\alpha u' - a \frac{Re_f g^*}{12K} \frac{\tau}{\tau+1} \left(\frac{l_t}{\delta_l^0}\right)^2 s_l^0 \right) \tag{6.17}$$

where a model constant a is introduced to take into account the various limitations of the simplified analysis proposed here.

A comparison of equations (2.1), (6.6) and (6.17) shows that the effect of a constant acceleration Γ may be modelled by adding a buoyancy slip velocity ΔU_s^b to the slip

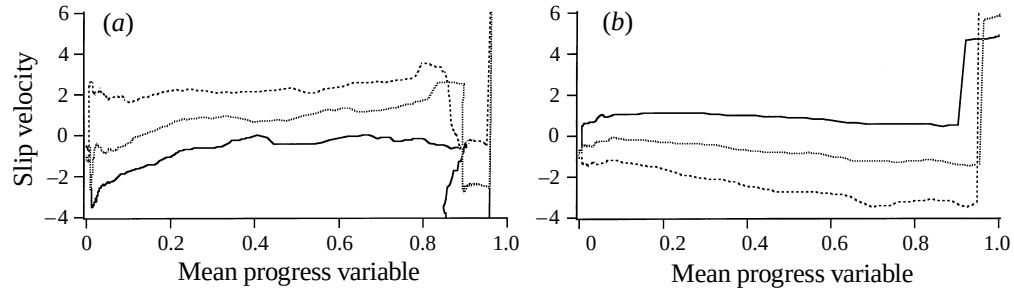

FIGURE 15. Slip velocity $(\overline{u}_{1b} - \overline{u}_{1u})$ plotted as a function of the mean progress variable $\widetilde{c}$ for various values of the reduced acceleration g^*. (*a*) Initial turbulent level $u'_0/s_l^0 = 5$: cases A (———), B (·····) and C (– – – –); (*b*) initial turbulent level $u'_0/s_l^0 = 2$: cases D (———), E (·····) and F (– – – –). Velocity is non-dimensionalized using the laminar flame speed s_l^0. Profiles are plotted for a reduced time $ts_l^0/\delta_l^0 = 2.7$.

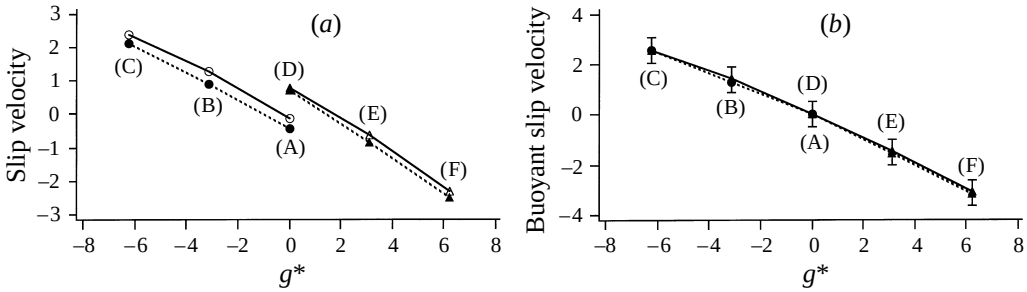

FIGURE 16. (*a*) Slip velocity $[\overline{u}_{1b} - \overline{u}_{1u}]$ $\left(\widetilde{c} = 0.5\right)$ and (*b*) buoyancy slip velocity ΔU_s^b estimated from expression (6.19), are plotted as a function of the reduced acceleration g^* for two reduced time steps $ts_l^0/\delta_l^0 = 2.1$ (———) and $ts_l^0/\delta_l^0 = 2.7$ (– – – –) and cases A to F. Error bars in (*b*) provide an estimation of numerical uncertainties. Velocity is non-dimensionalized using the laminar flame speed s_l^0.

velocity $(\overline{u}_{1b} - \overline{u}_{1u})$ obtained without imposed acceleration $(g^* = 0)$, where

$$\Delta U_s^b = -a \frac{Re_f g^*}{12K} \frac{\tau}{\tau + 1} \left(\frac{l_t}{\delta_l^0} \right)^2 s_l^0. \tag{6.18}$$

This analysis is well supported by DNS data as shown in figure 15 where the slip velocity $(\overline{u}_{1b} - \overline{u}_{1u})$, extracted from numerical data, is plotted as a function of the mean progress variable $\widetilde{c}$ for the six cases (A–F). The slip velocity is almost constant for a mean progress variable $\widetilde{c}$ lying between 0.1 and 0.8. In the following, this constant will be estimated using the value of the slip velocity for $\widetilde{c} = 0.5$. For mean progress variable values close to $\widetilde{c} = 0$ or $\widetilde{c} = 1$, the slip velocity is affected by sampling problems. In fact, when $\widetilde{c}$ is close to 0 (respectively 1), few samples are available to estimate $\overline{u}_{1b}$ (respectively $\overline{u}_{1u}$), the mean conditional velocity in burnt (respectively fresh) gases.

Negative values of the acceleration g^* (cases B and C) tend to increase ΔU_s^b and the slip velocity $(\overline{u}_{1b} - \overline{u}_{1u})$ and promote counter-gradient diffusion as expected from (2.1). On the other hand, positive accelerations (cases E and F) tend to decrease ΔU_s^b and $(\overline{u}_{1b} - \overline{u}_{1u})$ and promote gradient turbulent transport. The change in slip velocity seems to be a linear function of g^*. This point is analysed on figure 16(*a*) where the

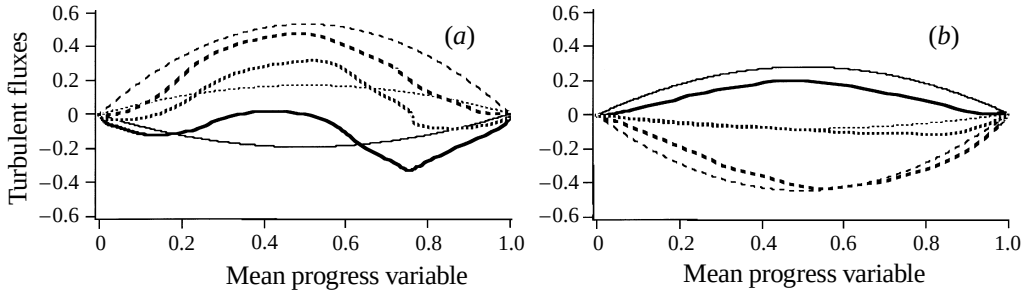

FIGURE 17. Comparison between DNS data (bold curves) and model predictions (thin curves) from (6.17) of the turbulent flux $\widetilde{u_1''c''}$ as a function of the mean progress variable $\widetilde{c}$ at reduced time 2.1 for cases: (*a*) A (———), B (– – – –), C (— — —); (*b*) D (———), E (– – – –), F(— — —). $\alpha = 0.5$, $a = 0.1$ and $K = 0.8$. The characteristic length l is taken equal to the integral length scale l_t. Velocity is non-dimensionalized using the laminar flame speed s_l^0.

value of the slip velocity $(\overline{u}_{1b} - \overline{u}_{1u})$ for $\widetilde{c} = 0.5$ is plotted as a function of g^* for two time steps and the six cases (A–F). A linear decrease of $(\overline{u}_{1b} - \overline{u}_{1u})_{\widetilde{c}=0.5}$ with g^* is observed. While the slope seems to be independent of the case considered, values of the slip velocity depend both on the case and the time step considered. All values in figure 16 collapse on a single line when only the buoyant slip velocity ΔU_s^b, estimated as

$$\Delta U_s^b = \left[(\overline{u}_{1b} - \overline{u}_{1u}) - (\overline{u}_{1b} - \overline{u}_{1u})_{g^*=0}\right] (\widetilde{c} = 0.5), \tag{6.19}$$

is plotted, as displayed on figure 16(*b*), showing a clear linear dependence of ΔU_s^b on the reduced acceleration g^*, as expected from (6.18). From figure 16(*a*) and assuming that $K = 0.8$, a may be estimated as $a = 0.1$.

Predictions from (6.17) are compared with simulation data for the reduced time 2.1 in figure 17. The efficiency function, α, is a function of the length-scale ratio l_t/δ_l and is obtained from previous DNS (Veynante *et al.* 1997) to be about 0.5 for the length-scale ratio used here. The agreement between numerical data and model predictions is satisfactory. The influence of the imposed acceleration and the transition between gradient and counter-gradient transport are well predicted from (6.17).

The same analysis may be extended to the case of an externally imposed pressure gradient $\partial\overline{P}/\partial x$, leading to a buoyant velocity

$$U_B(\widetilde{c}) \approx \frac{\tau}{12\rho_u \nu_u} \frac{Vl}{S} \left(\frac{\partial \overline{P}}{\partial x}\right) \left[\left(1 + (\tau+1)^{1-n}\right)\widetilde{c} - 1\right]. \tag{6.20}$$

The turbulent flux may then be expressed as

$$\widetilde{u_1''c''} = \widetilde{c}(1-\widetilde{c})\left(\tau s_l^0 - 2\alpha u' - a\frac{\tau^2 Re_f}{12K}\left(\frac{l_t}{\delta_l^0}\right)^2 \nabla p^* s_l^0\right) \tag{6.21}$$

where

$$\nabla p^* = \left(\frac{\partial \overline{P}}{\partial x}\right) \frac{\delta_l}{\rho_u \tau s_l^2} \tag{6.22}$$

is the reduced pressure gradient (i.e. the pressure gradient non-dimensionalized by the pressure gradient across the corresponding laminar flame).

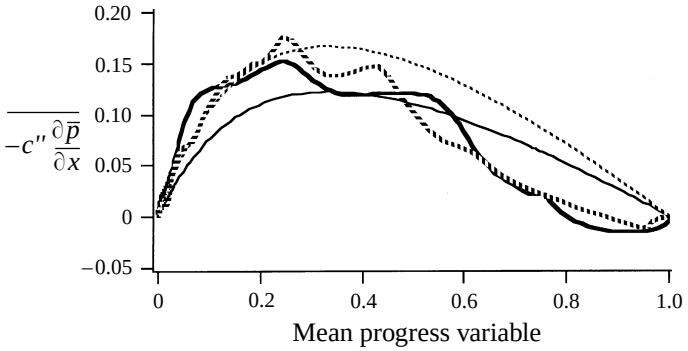

FIGURE 18. Pressure gradient terms $\overline{c''\partial p/\partial x}$ plotted as a function of the mean progress variable $\widetilde{c}$. Cases A (———) and D (– – – –). Bold lines correspond to DNS data. Thin lines correspond to the modelled sum of the thermal expansion (6.25) and the turbulent (6.27) contributions with $C_1 = 0.6$ and $C_2 = 0.25$. Pressure gradients are non-dimensionalized using $\rho_u \tau \left(s_l^0\right)^2 / \delta_l^0$. Reduced time is $ts_l^0/\delta_l^0 = 2.1$.

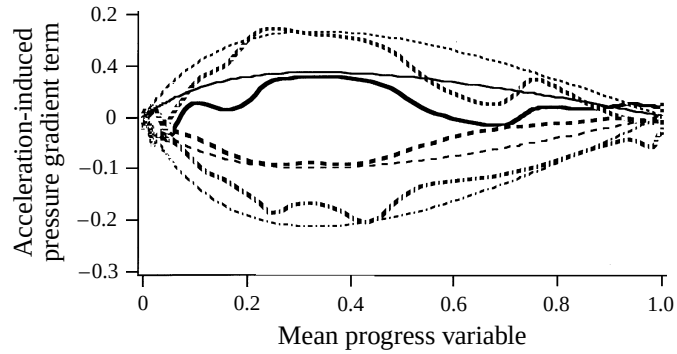

FIGURE 19. Acceleration-induced pressure gradient term, $-\left[\overline{c''\partial p/\partial x}|_{g^*} - \overline{c''\partial p/\partial x}|_{g^*=0}\right]$ plotted as a function of the mean progress variable $\widetilde{c}$. Cases B (———), C (– – – –), E (— — —) and F (— · —). Bold lines correspond to DNS data and thin lines to model expression (6.26), using $C_1 = 0.6$. Pressure gradients are non-dimensionalized using $\rho_u \tau \left(s_l^0\right)^2 / \delta_l^0$. Reduced time is $ts_l^0/\delta_l^0 = 2.1$.

6.3. *Analysis of the pressure terms in the balance equation for* $\overline{\rho}\widetilde{u''c''}$

The objective is now to propose a simple analysis of the pressure gradient terms (VI+VII), $\overline{c''\partial p/\partial x}$ in the balance equation (2.4) for the turbulent fluxes $\overline{\rho}\widetilde{u''c''}$. Pressure gradient terms for cases A and D, without any externally imposed acceleration, are plotted on figure 18 as a function of the mean progress variable $\widetilde{c}$. Although the turbulence level and the flame brush thickness are greater in case A than in case D, $\overline{c''\partial p/\partial x}$ is similar in the two cases, showing that the pressure gradient is mainly controlled by thermal expansion in these two simulations. On the other hand, the acceleration-induced pressure term, estimated as $\overline{c''\partial p/\partial x}|_{g^*} - \overline{c''\partial p/\partial x}|_{g^*=0}$ is mainly proportional to the imposed acceleration g^* as shown on figure 19.

The pressure gradient may be viewed as the sum of three contributions: the pressure gradient imposed by the laminar flame, ∇P_{lam}, the externally imposed pressure gradient, ∇P_{ext} and the pressure gradient induced by turbulent motions, ∇P_{turb}. Following this simple analysis, the pressure gradient term, $\overline{c''\partial p/\partial x}$ may be split in three contributions:

a buoyancy contribution due to thermal expansion and governed by the pressure gradient ∇P_{lam} imposed by the laminar flame front;

a buoyancy contribution due to the imposed acceleration (and/or imposed pressure gradient ∇P_{ext}) and probably governed by the buoyancy induced slip velocity ΔU_s^b previously introduced;

a turbulent contribution: from figure 18, this contribution seems to be negligible for cases A and D but may become important when the two buoyancy velocities tend to cancel each other out, a situation encountered in case F.

Then

$$-\overline{c''\frac{\partial p}{\partial x}} = -\overline{c''\frac{\partial p}{\partial x}}\bigg|_{flame} - \overline{c''\frac{\partial p}{\partial x}}\bigg|_{\nabla P_{ext}} - \overline{c''\frac{\partial p}{\partial x}}\bigg|_{turb}. \tag{6.23}$$

Each of these terms may be modelled as follows. Starting from the one-dimensional steady-state momentum balance equation in the flame framework:

$$\frac{\partial}{\partial x}\left(\rho u^2\right) = -\frac{\partial p}{\partial x} \tag{6.24}$$

where viscous effects are neglected, the pressure gradient term due to the flame may be estimated as

$$-\overline{c''\frac{\partial p}{\partial x}}\bigg|_{flame} = -\overline{c''\,\nabla P_{lam}} \approx C_1\,\overline{c''}\,\frac{\rho_u s_l^0 \Delta U_s^{th}}{\delta_l^0} = C_1\,\tau\,\frac{\widetilde{c}\,(1-\widetilde{c})}{1+\tau\widetilde{c}}\,\frac{\rho_u \tau\left(s_l^0\right)^2}{\delta_l^0} \tag{6.25}$$

where $\Delta U_s^{th} = \tau s_l^0$ is the slip velocity induced by the thermal expansion and C_1 is a model constant.

Viewing the acceleration term in the momentum equation as an equivalent buoyancy velocity ΔU_s^b leads to the contribution due to the constant acceleration:

$$-\overline{c''\frac{\partial p}{\partial x}}\bigg|_{\nabla P_{ext}} = -\overline{c''\,\nabla P_{ext}} \approx C_1\,\tau\,\frac{\widetilde{c}\,(1-\widetilde{c})}{1+\tau\widetilde{c}}\,\frac{\rho_u s_l^0 \Delta U_s^b}{\delta_l^0} \tag{6.26}$$

where the buoyancy slip velocity ΔU_s^b replaces the thermal expansion slip velocity $\Delta U_s^{th} = \tau s_l^0$. Estimates from (6.26) are plotted on figure 19 using $C_1 = 0.6$. The agreement with DNS data is very good.

The contribution due to turbulent motions is more difficult to estimate. In a first step, the following expression is proposed:

$$-\overline{c''\frac{\partial p}{\partial x}}\bigg|_{turb} \approx \overline{c''}\,\frac{\partial}{\partial x}\left(\overline{\rho}\widetilde{u''^2}\right) \approx -C_2\,\rho_u\,\tau\,\frac{\widetilde{c}\,(1-\widetilde{c})}{1+\tau\widetilde{c}}\,\frac{\overline{u'^2}}{l_t}. \tag{6.27}$$

This expression is based on the assumption that turbulent fluctuations are negligible in the burnt gases compared to the turbulent fluctuations u' in the fresh gases. The integral length scale l_t is used as an estimate of the flame brush thickness and C_2 is a model constant. The sum of the two contributions (6.25) and (6.27) are plotted on figure 18 for cases A and D using $C_2 = 0.25$. Even though (6.27) probably slightly overestimates the turbulent contribution, the agreement with DNS data is satisfactory.

A final estimate, adding the three previous contributions, is then

$$-\overline{c''\frac{\partial p}{\partial x}} \approx \rho_u \frac{(s_l^0)^2}{\delta_l^0}\tau\,\frac{\widetilde{c}\,(1-\widetilde{c})}{1+\tau\widetilde{c}}\left[C_1\left(\tau + \frac{\Delta U_s^b}{s_l^0}\right) - C_2\left(\frac{\overline{u'}}{s_l^0}\right)^2\frac{\delta_l^0}{l_t}\right]. \tag{6.28}$$

In (6.28), the contribution of the pressure terms in the balance equation for the

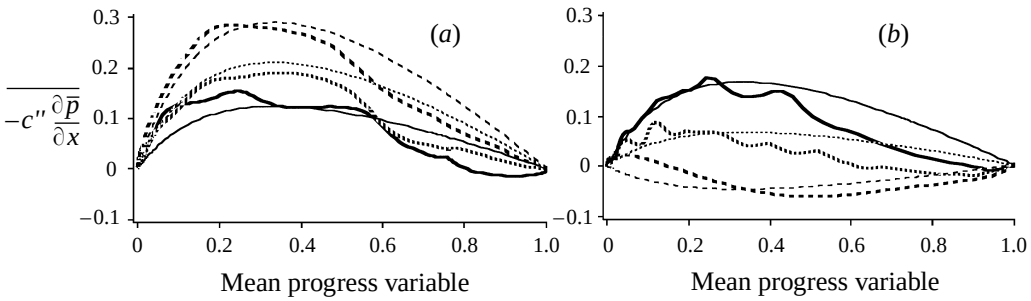

FIGURE 20. Comparison between DNS data (bold curves) and model predictions (thin curves) from (6.28) of the term $-\overline{c''\partial p/\partial x}$ plotted as a function of the mean progress variable $\widetilde{c}$ at reduced time $ts_l^0/\delta_l^0 = 2.1$ for cases: (*a*) A (———), B (– – – –), C (— — —); (*b*) D (———), E (– – – –), F(— — —). The model constants are $C_1 = 0.6$ and $C_2 = 0.25$. Pressure gradients are non-dimensionalized using $\rho_u \tau \left(s_l^0\right)^2 / \delta_l^0$.

turbulent fluxes $\overline{\rho}\widetilde{u_i''c''}$ is split in two components. The first one is described in terms of slip velocity and incorporates buoyancy effects due to the thermal expansion and to externally imposed pressure gradients. The second part compares turbulence levels in burnt and fresh gases. A similar analysis may also be conducted to estimate the mean pressure gradient $\partial\overline{p}/\partial x$. As the buoyancy slip velocity is proportional to the imposed constant acceleration Γ (see (6.15)), the mean pressure gradient is also a linear function of Γ as expected from (2.7).

The simple model (6.28) may be improved in various ways but is found to be in good agreement with numerical data as shown on figure 20.

6.4. *Discussion*

In the previous section, a simple model, based on the assumption of an equilibrium between buoyancy and drag forces acting on a pocket of fresh gases (respectively burnt gases) in a medium of burnt (respectively fresh) gases, was derived to describe the change in turbulent transport induced by a constant acceleration (or a constant pressure gradient). Two other descriptions of the same phenomenon may be found in the literature. These approaches are now briefly summarized and discussed.

6.4.1. *The Chomiak & Nisbet analysis*

In a recent paper, Chomiak & Nisbet (1995) propose an analysis based on arguments similar to the one presented in §6.2. The main difference lies in the description of the velocities U_B^u (respectively U_B^b) induced by buoyancy effects on a pocket of fresh (burnt) gases in a medium of burnt (fresh) gases. For Chomiak & Nisbet (1995), the analysis derived in §6.2 is too crude: pockets of gases cannot be assumed to move as solid bodies under buoyancy forces because of pocket deformations. Accordingly, they propose for a pocket of size l_t and density ρ_0 in a medium of density ρ_∞ expressing the buoyancy-induced velocity u as

$$u^2 = 0.09 \left(\frac{\Gamma l_t \left| 1 - \rho_0/\rho_\infty \right|}{\alpha} \right) \tag{6.29}$$

where α is the entrainment coefficient, depending on how the pockets are organized during the starting period. For a fully developed turbulent flow, a value $\alpha \approx 0.4$ is

retained. Then, (6.10) and (6.11) may be recast as

$$U_B^b \approx -b\left(l_t|\Gamma|\frac{\tau}{\tau+1}\right)^{1/2}, \tag{6.30}$$

$$U_B^u \approx b\left(l_t|\Gamma|\tau\right)^{1/2} \tag{6.31}$$

where b is a model constant having the same sign as the acceleration Γ.

Assuming as previously (equation (6.12)) a linear variation of the buoyancy velocity $U_B(\widetilde{c})$ with the mean progress variable $\widetilde{c}$ leads to

$$U_B(\widetilde{c}) \approx b\left(\widetilde{c}-\frac{1}{1+(\tau+1)^{1/2}}\right)\left(1+\frac{1}{(\tau+1)^{1/2}}\right)\left(|\Gamma|l_t\tau\right)^{1/2}, \tag{6.32}$$

Which may be recast as

$$U_B(\widetilde{c}) \approx b\left(\widetilde{c}-K\right)\left(1+\frac{1}{(\tau+1)^{1/2}}\right)\left(|\Gamma|l_t\tau\right)^{1/2} \tag{6.33}$$

leading to a simple expression for the turbulent flux $\widetilde{u_1''c''}$:

$$\widetilde{u_1''c''} = \widetilde{c}\left(1-\widetilde{c}\right)\left[\tau s_l^0 - 2\alpha u' - b\left(1+\frac{1}{(\tau+1)^{1/2}}\right)\left(\tau|g^*|\frac{l_t}{\delta_l^0}\right)^{1/2} s_l^0\right]. \tag{6.34}$$

The scaling of the buoyancy-induced slip velocity ΔU_s^b is different from the one introduced in §6.2. In the Chomiak & Nisbet (1995) analysis, the effect of buoyancy is linearly dependent on the square roots of the acceleration g^* and the length-scale ratio l_t/δ_l^0. In our analysis, buoyancy effects are linearly related to g^* and $(l_t/\delta_l^0)^2$. The Chomiak & Nisbet analysis is not sustained by our DNS results (figure 16(*b*)) where a linear dependence of buoyancy effects g^* is found. Further investigations are required concerning the length-scale ratio dependence.

6.4.2. *The Bray, Moss & Libby analysis*

The Bray, Moss & Libby (1982) analysis is based on a different approach. Starting from the exact transport equation for the turbulent fluxes $\overline{\rho}\widetilde{u_i''c''}$, (2.4), the authors assume, for large mean pressure gradients, an equilibrium between the mean pressure gradient term (VI) and dissipation terms (VIII + IX). Then, from modelling considerations, they propose a buoyancy-induced slip velocity as,

$$\Delta U_B^s = -\frac{\tau l_t}{\rho_u u'}\frac{\partial \overline{p}}{\partial x}, \tag{6.35}$$

which may be recast as

$$\Delta U_B^s = -\tau^2\frac{l_t}{\delta_l^0}\frac{s_l^0}{u'}\nabla p^* s_l^0 = -\tau^2 D_a \nabla p^* s_l^0 \tag{6.36}$$

where the reduced pressure gradient ∇p^* is given by (6.22). D_a is the Damköhler number and compares turbulent and chemical time scales. Following Bray (1990), the ratio $l_t s_l^0/u'$ may be viewed as a flame wrinkling length scale L_y.

Comparing this expression with our analysis (6.21) and DNS results leads to several comments.

(i) The two expressions exhibit the same scaling in pressure gradient ∇p^* (or in acceleration g^*) and in heat release factor τ. Nevertheless, our expression predicts

Case	u'_0/s^0_l	l_t/δ^0_l	g^*	GD/CGD	N^Γ_B
A	5	3.5	0	GD	0.60
B	5	3.5	−3.12	transition	0.95
C	5	3.5	−6.25	CGD	1.3
D	2	3.5	0	CGD	1.5
E	2	3.5	3.12	GD	0.60
F	2	3.5	6.25	GD	−0.25

TABLE 4. Estimation of N^Γ_B. GD (CGD) refers to gradient (counter-gradient) turbulent diffusion.

an evolution proportional to $(l_t/\delta^0_l)^2$ against a linear evolution with l_t/δ^0_l in (6.36). Bray *et al.* point out that their expression may be recovered by writing an equilibrium between buoyancy and drag forces, assuming a drag coefficient C_x inversely proportional to the velocity. In our analysis, the drag coefficient is assumed to be inversely proportional to the Reynolds number (Stokes law) and accordingly inversely proportional to the velocity and the length scale l.

(ii) The dependence of ΔU^s_B on u' predicted from (6.36) should induce a change by a factor of about 2 in the slope of the curve on figure 16(*b*) between cases A–C and D–F. Such a change is not observed in our DNS.

(iii) The Bray *et al.* analysis is developed assuming an equilibrium between the mean pressure gradient term (VI) and the dissipation terms (VIII + IX) in (2.4). This assumption is clearly not validated by our DNS data showing that the pressure fluctuation term (VII) cannot be neglected, at least when a constant acceleration is imposed (see §5.4).

6.5. *A criterion for gradient/counter-gradient turbulent diffusion*

A simple criterion may be derived to predict the occurrence of counter-gradient turbulent diffusion (i.e. $\widetilde{u''_1 c''} \geqslant 0$) for flames subjected to a constant acceleration g^*, from (6.17):

$$N^\Gamma_B = \frac{\tau}{2\alpha u'/s^0_l}\left[1 - a\frac{g^* Re_f}{12K\,(\tau+1)}\left(\frac{l}{\delta_l}\right)^2\right] \geqslant 1. \tag{6.37}$$

The effect of the constant acceleration is to introduce a correction to the criterion (1.3) N_B defined by Veynante *et al.* (1997).

This modified criterion may be estimated from our numerical simulation, using the initial turbulence values ($l = l_t$, $u' = u'_0$), $\alpha = 0.5$ (from Veynante *et al.* 1997), $a = 0.12$ and $K = 0.8$. Results are summarized and validated in table 4: it appears that $N^\Gamma_B \geqslant 1$ flows indeed exhibit counter-gradient diffusion.

For flames subjected to constant pressure gradients, (6.21) leads to the following criterion for counter-gradient turbulent transport:

$$N^p_B = \frac{\tau}{2\alpha u'/s^0_l}\left[1 - a\frac{\tau \nabla p^* Re_f}{12K}\left(\frac{l}{\delta_l}\right)^2\right] \geqslant 1 \tag{6.38}$$

where

$$\nabla p^* = \left(\frac{\partial \overline{P}}{\partial x}\right)\frac{\delta_l}{\rho_u \tau s_l^2} \tag{6.39}$$

which is the reduced pressure gradient (i.e. the pressure gradient non-dimensionalized by the pressure gradient across the corresponding laminar flame).

Case	N_B^p	$\overline{\rho}\widetilde{u_1''c''}/\overline{\rho}\widetilde{U}_0$
unconfined	0.9	0.0043
confined	20	0.051

TABLE 5. Estimation of N_B^p in the Shepherd *et al.* (1982) experiment for the confined (with pressure gradients) and unconfined (without pressure pressure gradients) flames. Experimental estimations of $\overline{\rho}\widetilde{u_1''c''}/\overline{\rho}\widetilde{U}_0$, where $\widetilde{U}_0$ is the reference burner inlet velocity, are provided. $u' \approx 1$ m s^{-1}, $l_t \approx 1$ cm. Owing to the large length-scale ratio l_t/δ_l^0, the efficiency function α is estimated as $\alpha \approx 1$ (Veynante *et al.* 1997).

Shepherd *et al.* (1982) performed experiments on 'free' flames ($\nabla P_{ext} = 0$) and on ducted flames (with a favourable pressure gradient $\nabla P_{ext} = 1000$ Pa m^{-1}). Their measurements of $\overline{\rho}\widetilde{u''c''}$ are summarized in table 5 and their trend is well predicted by the above criterion: the number N_B for the free flame is 0.9 and is close to the transition between gradient and counter-gradient turbulent diffusion. The experiment reveals that a small counter-gradient diffusion flux exists in this flame. However, the confined flame has a number N_B^P of 20 and experimental diffusion fluxes are indeed large and controlled by counter-gradient turbulent transport.

7. Conclusion

The influence of a constant acceleration Γ on a turbulent premixed flame has been studied by direct numerical simulation. This acceleration Γ induces a mean pressure gradient across the flame brush, leading to a modification of the turbulent flame structure due to differential buoyancy mechanisms between heavy cold fresh and light hot burnt gases. Such a pressure gradient is encountered in practical applications, for example in ducted flames.

A favourable pressure gradient, i.e. a pressure decrease from unburnt to burnt gases, is found to decrease flame wrinkling, flame brush thickness, and turbulent flame speed. A favourable pressure gradient also promotes counter-gradient turbulent transport. On the other hand, adverse pressure gradients tend to increase the flame brush thickness and turbulent flame speed, and promote classical gradient turbulent transport. As proposed by Libby (1989), the turbulent flame speed is modified by a buoyancy term linearly dependent on the imposed constant acceleration Γ and on the integral length scale l_t.

The balance equation for the turbulent flux $\overline{\rho}\widetilde{u''c''}$ of the Favre-averaged progress variable $\overline{c}$ is also analysed. The first results show that the fluctuating pressure term, $(\overline{c''\partial p'/\partial x})$, cannot be neglected as generally assumed in models, at least when a constant acceleration is imposed. Simple models assuming that a high mean pressure gradient may only be balanced by the cross-dissipation term seem too approximate. In fact, the mean pressure term $\overline{c}''\partial\overline{p}/\partial x$ and the fluctuating pressure term $\overline{c''\partial p'/\partial x}$ have to be modelled together as $\overline{c''\partial p/\partial x}$. A first analysis is proposed but will need to be continued to compare simulation data and closure schemes proposed for the $\overline{\rho}\widetilde{u''c''}$ transport equation.

The analysis developed by Veynante *et al.* (1997) has been extended to flows with imposed acceleration and mean pressure gradients. A simple model for the turbulent flux $\widetilde{u''c''}$ is proposed, validated from simulation data and compared to existing models of Chomiak & Nisbet (1995) and Bray–Moss–Libby. The influence of the

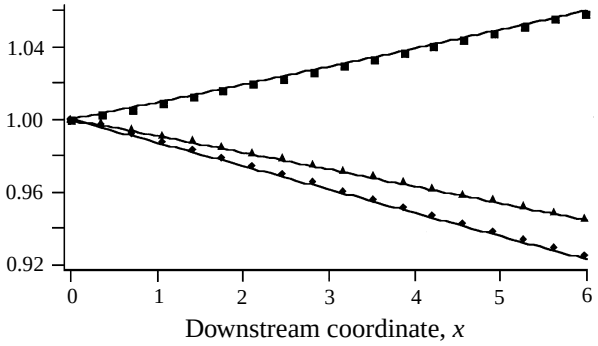

FIGURE 21. Tests of code for one-dimensional flow with constant volume force $F_v/\rho_0 c_0^2 = 0.01$. Comparison between simulation data: velocity (■), pressure (◆), density (▲) and analytical results (———) plotted as a function of the reduced downstream coordinate x. Quantities are non-dimensionalized by their values for $x = 0$.

length-scale ratio l_t/δ_l^0 comparing the turbulent integral length scale and the laminar flame thickness remains to be investigated. Then, a modified criterion will need to be derived to delineate between counter-gradient and gradient turbulent diffusion. In fact, counter-gradient diffusion may occur in most practical applications, especially for ducted flames.

The authors acknowledge the support of their home institutions (Centre National de la Recherche Scientifique, Ecole Centrale Paris and Institut de Mecanique des Fluides de Toulouse) during their stay at the Center for Turbulence Research. Computations were partially performed at IDRIS (Institut de Developpement et de Ressources en Informatique Scientifique), the French national computing center of CNRS. Dr A. Trouvé and Professor K.N.C. Bray also provided valuable inputs for this study. The post-processing tools were based on the initial work of Dr D. Haworth.

Appendix. Tests with constant force or acceleration

To validate the implementation of volume forces in the simulation, simple examples of one-dimensional flows with constant force or acceleration have been run. We consider an isentropic one-dimensional flow submitted to a force F_v; F_v is either constant or equal to $\rho\gamma$. The governing equations are

$$\frac{\partial(\rho u)}{\partial x} = 0, \quad \frac{\partial(\rho u^2 + p)}{\partial x} = F.$$

For constant volume force F_v, F is constant and equal to F_v and for constant acceleration, $F = \rho\Gamma$.

This system is integrated once to give

$$\rho u = \rho_0 u_0,$$

$$\frac{\partial u}{\partial x} = -\frac{u_0}{c_o^2 \rho_0} \frac{F}{(u_0/u)^{\gamma+1}(1 - M_0^2(u/u_0)^{\gamma+1})}$$

where index 0 designates the inlet condition. $M_0 = u_0/c_0$ is the inlet Mach number and $\gamma = 1.4$.

If the Mach number M_0 is small, this system may be integrated easily to give:

for constant volume force F_v:

$$u(x) = u_0 \left(1 - \frac{F_v x}{P_0}\right)^{-1/\gamma}, \quad \rho(x) = \rho_0 \left(1 - \frac{F_v x}{P_0}\right)^{1/\gamma}, \quad P(x) = P_0 - F_v x;$$

note that $\partial P/\partial x = -F_v$;

for constant acceleration Γ:

$$u(x) = u_0 \left(1 + \frac{(\gamma - 1)\Gamma x}{c_0^2}\right)^{-1/(\gamma-1)},$$

$$\rho(x) = \rho_0 \left(1 + \frac{(\gamma - 1)\Gamma x}{c_0^2}\right)^{1/(\gamma-1)},$$

$$P(x) = P_0 \left(1 + \frac{(\gamma - 1)\Gamma x}{c_0^2}\right)^{\gamma/(\gamma-1)}$$

where c_0 is the inlet sound speed ($c_0 = \gamma P_0/\rho_0$).

For small values of Γ, $\partial P/\partial x = \rho_0 \Gamma$.

Figure 21 shows (for a constant volume force $F_v/\rho_0 c_0^2 = 0.01$) that the simulation results match these analytical expressions well. (A similar agreement is obtained in the case of a constant acceleration.)

REFERENCES

Batchelor, G. K. 1967 *Introduction to Fluid Dynamics*. Cambridge University Press.

Bray, K. N. C. 1980 Turbulent flows with premixed reactants. In *Turbulent Reacting Flows* (ed. P. A. Libby & F. A. Williams). Topics in Applied Physics, vol. 44, pp. 115–183. Springer.

Bray, K. N. C. 1990 Studies of the turbulent burning velocity. *Proc. R. Soc. Lond.* A **431**, 315–335.

Bray, K. N. C., Champion, M. & Libby, P. A. 1989 The interaction between turbulence and chemistry in premixed turbulent flames. In *Turbulent Reactive Flows* (ed. R. Borghi & S. N. B. Murthy). Lecture Notes in Engineering, vol. 40, pp. 541–563. Springer.

Bray, K. N. C., Libby, P. A., Masuya, G. & Moss, J. B. 1981 Turbulence production in premixed turbulent flames. *Combust. Sci. Tech.* **25**, 127–140.

Bray, K. N. C., Moss, J. B. & Libby, P. A. 1982 Turbulence transport in premixed turbulent flames. In *Convective Transport and Instability Phenomena* (ed. J. Zierep & H. Oertel). University of Karlsruhe, Germany.

Chomiak, J. & Nisbet, J. R. 1995 Modeling variable density effects in turbulent flames - some basic considerations. *Combust. Flame* **102**, 371–386.

Haworth, D. C. & Poinsot, T. 1992 Numerical simulations of Lewis number effects in turbulent premixed flames. *J. Fluid Mech.* **244**, 405–436.

Libby, P. A. 1989 Theoretical analysis of the effect of gravity on premixed turbulent flames. *Combust. Sci. Tech.* **68**, 15–33.

Libby, P. A. & Bray, K. N. C. 1981 Countergradient diffusion in premixed turbulent flames. *AIAA J.* **19**, 205–213.

Masuya, G. & Libby, P. A. 1981 Nongradient theory for oblique turbulent flames with premixed reactants. *AIAA J.* **19**, 1590–1599.

Moss, J. B. 1980 Simultaneous measurements of concentration and velocity in an open premixed turbulent flame. *Combust. Sci. Tech.* **22**, 119–129.

Poinsot, T. & Lele, S. K. 1992 Boundary conditions for direct simulations of compressible viscous flows. *J. Comput. Phys.* **101**, 104–129.

Poinsot, T., Veynante, D. & Candel, S. M. 1991 Quenching processes and premixed turbulent combustion diagrams. *J. Fluid Mech.* **228**, 561–605.

Rutland, C. J. & Cant, R. S. 1994 Turbulent transport in premixed flames. In *Proc. Summer Program*. Center for Turbulence Research, NASA Ames/Stanford University.

Shepherd, I. G., Moss, J. B. & Bray, K. N. C. 1982 Turbulent transport in a confined premixed flame. In *Nineteenth Symp. (Intl) on Combustion*, pp. 423–431. The Combustion Institute.

Trouvé, A., Veynante, D., Bray, K. N. C. & Mantel, T. 1994 The coupling between flame surface dynamics and species mass conservation in premixed turbulent combustion. In *Proc. Summer Program*, Center for Turbulence Research, NASA Ames/Stanford University.

Veynante, D., Trouvé, A., Bray, K. N. C. & Mantel T. 1997 Gradient and counter-gradient scalar transport in turbulent premixed flames. *J. Fluid Mech.* **332**, 263–293.

Williams, F. A. 1985 *Combustion Theory*, 2nd edn. Benjamin Cummings.